

Black Hole Binary Dynamics and Waveforms from Classical and Quantum Gravitational Scattering

Thibault Damour
Institut des Hautes Etudes Scientifiques

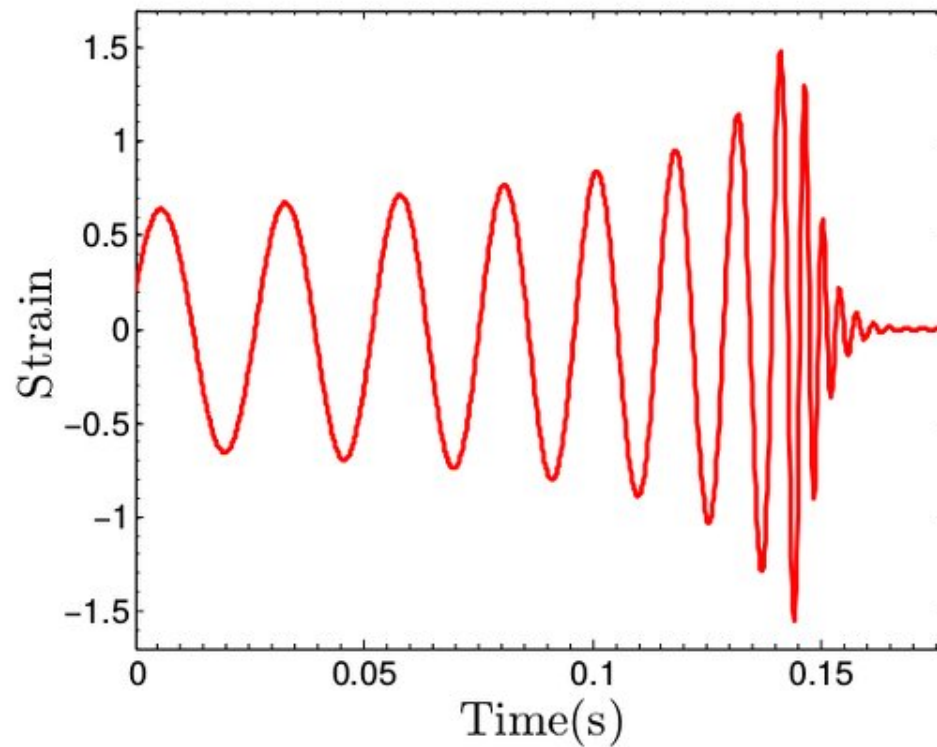
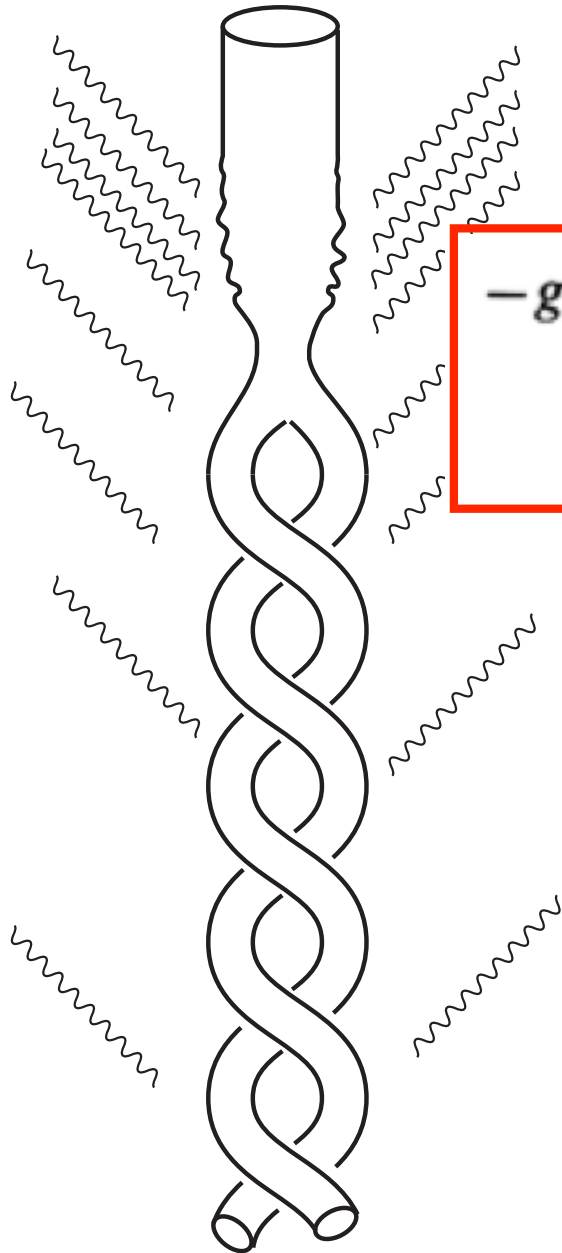


**Journées relativistes de Tours,
Institut Denis Poisson, Faculté de Grandmont
31 Mai-2 Juin 2023, Tours, France**

$$R_{\mu\nu} - \frac{1}{2}R g_{\mu\nu} = \frac{8\pi G}{c^4}T_{\mu\nu} \quad R_{\mu\nu} = 0$$

$$ds^2 = g_{\mu\nu}(x^\lambda) dx^\mu dx^\nu$$

$$-g^{\mu\nu} g_{\alpha\beta, \mu\nu} + g^{\mu\nu} g^{\rho\sigma} (g_{\alpha\mu, \rho} g_{\beta\nu, \sigma} - g_{\alpha\mu, \rho} g_{\beta\sigma, \nu} + g_{\alpha\mu, \rho} g_{\nu\sigma, \beta} + g_{\beta\mu, \rho} g_{\nu\sigma, \alpha} - \frac{1}{2} g_{\mu\rho, \alpha} g_{\nu\sigma, \beta}) = 0$$



Tools used for the GR 2-body pb

Post-Newtonian (PN) approximation (**expansion in $1/c$; ie v^2/c^2 and $GM/(c^2r)$**)

Post-Minkowskian (PM) approximation (**expansion in G ; ie in $GM/(c^2b)$**) and its recent **Worldline EFT avatars**

Multipolar post-Minkowskian (MPM) approximation theory to the GW emission of binary systems

Matched Asymptotic Expansions useful both for the motion of strongly self-gravitating bodies, and for the nearzone-wavezone matching

Gravitational Self-Force (SF): expansion in m_1/m_2 , with « first law of BH mechanics » (LeTiec-Blanchet-Whiting'12,...)

Effective One-Body (EOB) Approach

Numerical Relativity (NR)

Effective Field Theory (EFT)

Quantum scattering amplitude aided by Double-Copy, Generalized Unitarity, « Feynman-integral Calculus » (IBP, DE, regions, reverse unitarity,...), Kosower-Maybee-O'Connell

+ Worldline QFT

Tutti Frutti method

R
e
c
e
n
t

Post-Newtonian Expansion of the Reduced Gravity Action

2Post-Minkowskian (G^2 , one-loop) has been explicitly computed (Westpfahl et al. '79,'85; Bel-Damour-Deruelle-Ibanez-Martin'81) but, **at the time, classical PM calculations did not go beyond one-loop**

→ Use slow-motion-weak-field PN expansion: in powers of $1/c^2$:

1PN= $(v/c)^2$; 2PN= $(v/c)^4$, etc n PN= $(v/c)^{2n}$

$$\square^{-1} = \left(\Delta - \frac{1}{c^2} \partial_t^2 \right)^{-1} = \Delta^{-1} + \frac{1}{c^2} \partial_t^2 \Delta^{-2} + \dots$$

First Post-Newtonian=1PN= $G \left[(v/c)^2 + Gm/(r c^2) \right]$

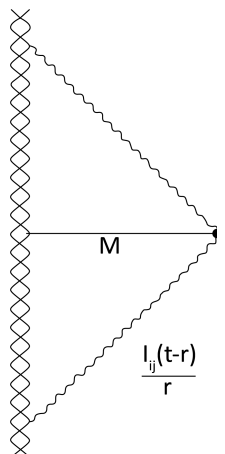
$$L^{(1)} = \sum_A -m_A c^2 \sqrt{1 - \frac{v_A^2}{c^2}} = \sum_A \left(-m_A c^2 + \frac{1}{2} m_A v_A^2 + \frac{1}{8c^2} m_A v_A^4 + \dots \right)$$

$$L^{(2)} = \frac{1}{2} \sum_{A \neq B} \frac{G_N m_A m_B}{r_{AB}} \left[1 + \frac{3}{2c^2} (v_A^2 + v_B^2) - \frac{7}{2c^2} (\mathbf{v}_A \cdot \mathbf{v}_B) - \frac{1}{2c^2} (\mathbf{n}_{AB} \cdot \mathbf{v}_A)(\mathbf{n}_{AB} \cdot \mathbf{v}_B) + O\left(\frac{1}{c^4}\right) \right]$$

$$L^{(3)} = -\frac{1}{2} \sum_{B \neq A \neq C} \frac{G_N^2 m_A m_B m_C}{r_{AB} r_{AC} c^2} + O\left(\frac{1}{c^4}\right)$$

Computed up to 4PN

includes tail-transported nonlocal effects
Blanchet-D88



$$H_{4PN}^{\text{nonloc}}(t) = -\frac{1}{5} \frac{G^2 M}{c^8} I_{ij}^{(3)}(t) \times \text{Pf}_{2r_{12}/c} \int_{-\infty}^{+\infty} \frac{dv}{|v|} I_{ij}^{(3)}(t+v),$$

GRAVITATIONAL WAVE GENERATION: MULTIPOLAR POST-MINKOWSKIAN

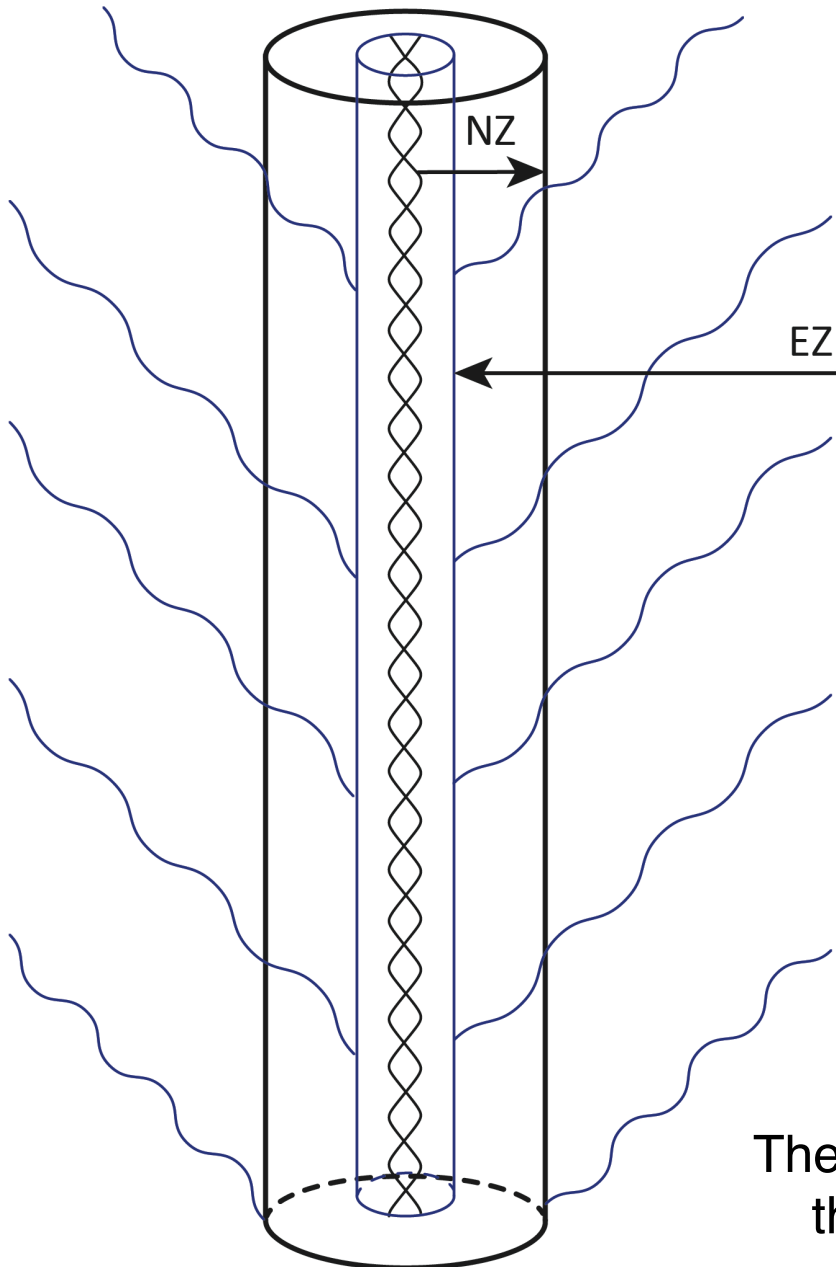
FORMALISM (BLANCHET-DAMOUR-IYER)

Decomposition of space-time in various overlapping regions:

1. **near-zone**: $r \ll \lambda$: PN
2. **exterior zone**: $r \gg r_{\text{source}}$: MPM
3. **far wave-zone**: Bondi-type expansion

then **matching between the zones**

in exterior zone, **iterative solution** of Einstein's vacuum field equations by means of a **double expansion** in non-linearity and in multipoles, with crucial use of **analytic continuation** (complex B) for dealing with formal UV divergences at $r=0$



$$\begin{aligned}
 g &= \eta + Gh_1 + G^2h_2 + G^3h_3 + \dots, \\
 \square h_1 &= 0, \\
 \square h_2 &= \partial\partial h_1 h_1, \\
 \square h_3 &= \partial\partial h_1 h_1 h_1 + \partial\partial h_1 h_2, \\
 h_1 &= \sum_{\ell} \partial_{i_1 i_2 \dots i_{\ell}} \left(\frac{M_{i_1 i_2 \dots i_{\ell}}(t - r/c)}{r} \right) + \partial\partial \dots \partial \left(\frac{\epsilon_{j_1 j_2 k} S_{k j_3 \dots j_{\ell}}(t - r/c)}{r} \right), \\
 h_2 &= FP_B \square_{\text{ret}}^{-1} \left(\left(\frac{r}{r_0} \right)^B \partial\partial h_1 h_1 \right) + \dots, \\
 h_3 &= FP_B \square_{\text{ret}}^{-1} \dots
 \end{aligned}$$

STF tensors encoding multipole moments

mass-type and spin-type multipole moments

The PN-matched MPM formalism has allowed to compute the GW emission to very high accuracy (Blanchet et al)

Perturbative computation of GW flux from binary system

- lowest order : Einstein 1918 Peters-Mathews 63
- $1 + (v^2/c^2)$: Wagoner-Will 76
- ... + (v^3/c^3) : Blanchet-Damour 92, Wiseman 93
- ... + (v^4/c^4) : Blanchet-Damour-Iyer Will-Wiseman 95
- ... + (v^5/c^5) : Blanchet 96
- ... + (v^6/c^6) : Blanchet-Damour-Esposito-Farèse-Iyer 2004
- ... + (v^7/c^7) : Blanchet
- ... + $(v^8/c^8) + (v^9/c^9)$: Blanchet et al 2023

$$\nu = \frac{m_1 m_2}{(m_1 + m_2)^2}$$

$$x = \left(\frac{v}{c}\right)^2 = \left(\frac{G(m_1 + m_2)\Omega}{c^3}\right)^{\frac{2}{3}} = \left(\frac{\pi G(m_1 + m_2)f}{c^3}\right)^{\frac{2}{3}}$$

LO
quadrupole
radiation

$$\mathcal{F} = \frac{32c^5}{5G} \nu^2 x^5 \left\{ 1 + \left(-\frac{1247}{336} - \frac{35}{12}\nu \right) x + 4\pi x^{3/2} + \left(-\frac{44711}{9072} + \frac{9271}{504}\nu + \frac{65}{18}\nu^2 \right) x^2 + \left(-\frac{8191}{672} - \frac{583}{24}\nu \right) \pi x^{5/2} \right.$$

$$+ \left[\frac{6643739519}{69854400} + \frac{16}{3}\pi^2 - \frac{1712}{105}\gamma_E - \frac{856}{105}\ln(16x) + \left(-\frac{134543}{7776} + \frac{41}{48}\pi^2 \right) \nu - \frac{94403}{3024}\nu^2 - \frac{775}{324}\nu^3 \right] x^3$$

$$+ \left(-\frac{16285}{504} + \frac{214745}{1728}\nu + \frac{193385}{3024}\nu^2 \right) \pi x^{7/2}$$

$$+ \left[-\frac{323105549467}{3178375200} + \frac{232597}{4410}\gamma_E - \frac{1369}{126}\pi^2 + \frac{39931}{294}\ln 2 - \frac{47385}{1568}\ln 3 + \frac{232597}{8820}\ln x \right.$$

$$+ \left(-\frac{1452202403629}{1466942400} + \frac{41478}{245}\gamma_E - \frac{267127}{4608}\pi^2 + \frac{479062}{2205}\ln 2 + \frac{47385}{392}\ln 3 + \frac{20739}{245}\ln x \right) \nu$$

$$+ \left(\frac{1607125}{6804} - \frac{3157}{384}\pi^2 \right) \nu^2 + \frac{6875}{504}\nu^3 + \frac{5}{6}\nu^4 \left. \right] x^4$$

$$+ \left[\frac{265978667519}{745113600} - \frac{6848}{105}\gamma_E - \frac{3424}{105}\ln(16x) + \left(\frac{2062241}{22176} + \frac{41}{12}\pi^2 \right) \nu \right.$$

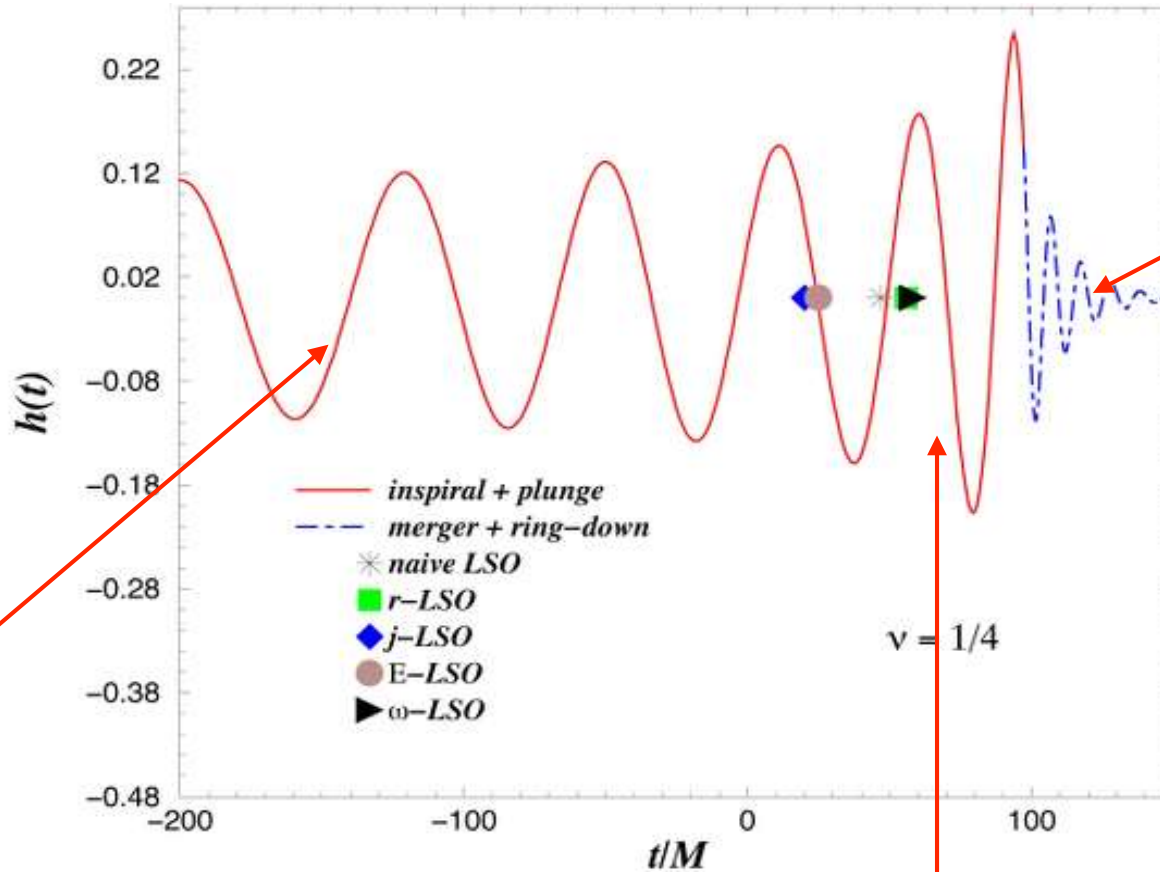
$$\left. - \frac{133112905}{290304}\nu^2 - \frac{3719141}{38016}\nu^3 \right] \pi x^{9/2} + \mathcal{O}(x^5) \left. \right\}. \quad (4)$$

4PN

4.5PN

The Effective One-Body (EOB) approach to the GW signal emitted by the Merger of two Black Holes

Buonanno-TD'2000



Ringdown (BBH):
 « vibration modes »
 of final BH (QNM);
 perturbation
 of BHs à la
 Regge-Wheeler-Zerilli-
 Teukolsky
 +Vishveshwara

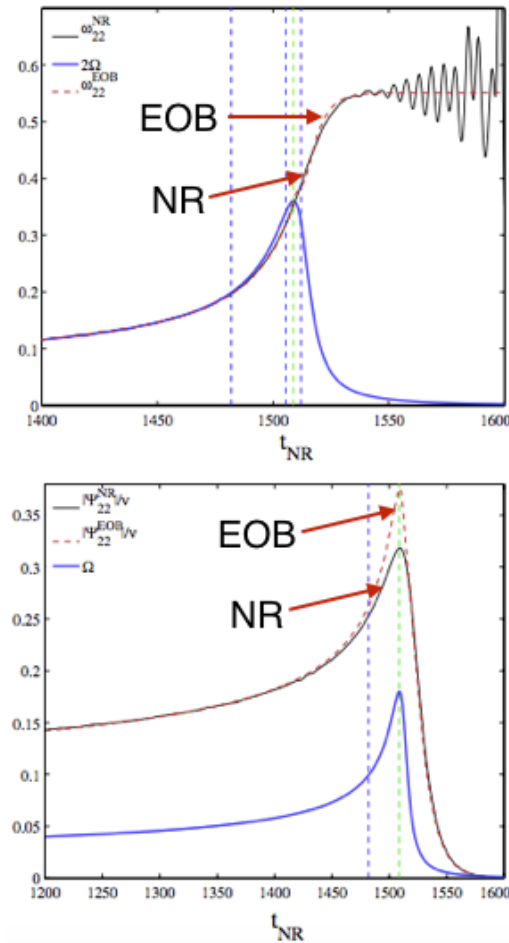
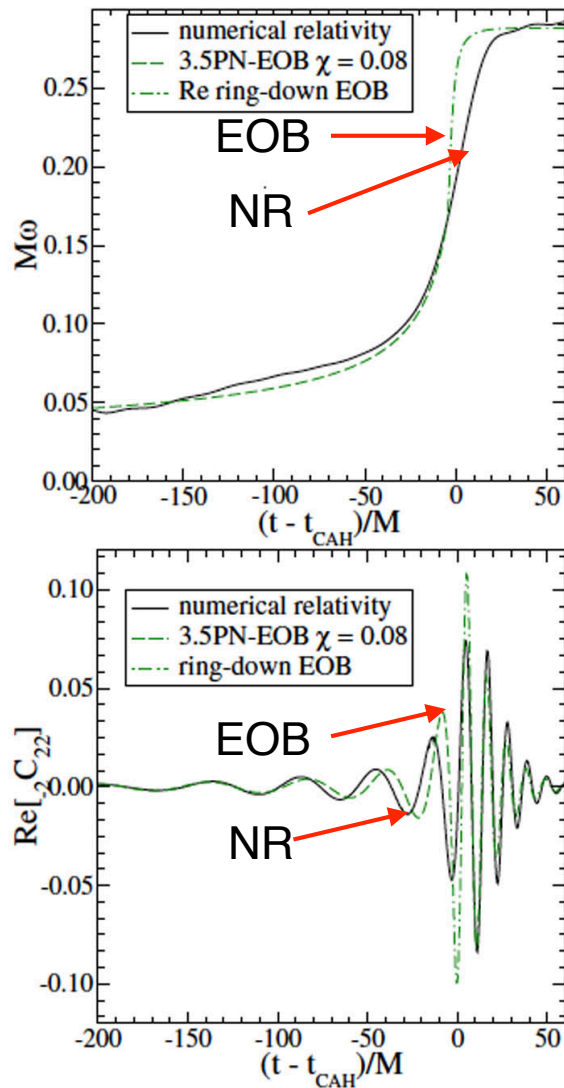
Inspiral:
 perturbative
 computation
 of higher-order
 contributions
 to $E=H$ and F
 (expansion in v^2/c^2
 tidal polarizability
 of NS)

Late inspiral, « plunge » and merger:
 first estimated by the Effective One-Body method (AB-TD 2000)
 later confirmed and improved by using
 numerical simulations (Pretorius...2005)

From EOB vs NR to EOB-NR waveforms

Buonanno-Cook-Pretorius 2007

TD-Nagar-Dorband-Pollney-Rezzolla 2008



EOB-NR vs NR

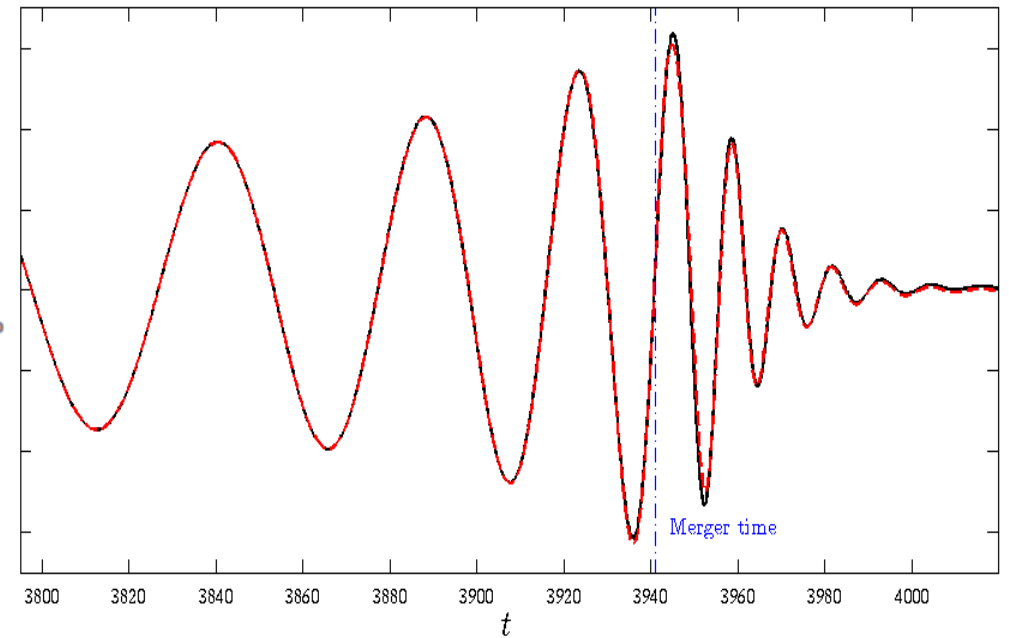


FIG. 21 (color online). We compare the NR and EOB frequency and $\text{Re}[{}_2C_{22}]$ waveforms throughout the entire inspiral-merger-ring-down evolution. The data refers to the $d = 16$ run.

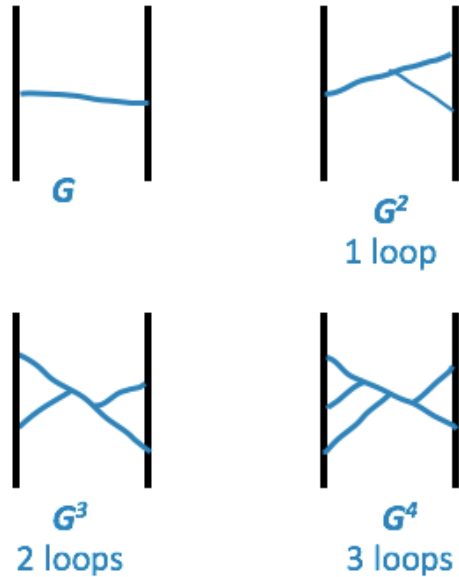
Effective One-Body (EOB) approach: H + Rad-Reac Force

Historically rooted in QM: Brezin-Itzykson-ZinnJustin'70
 eikonal scattering amplitude+ Wheeler's: 'Think quantum mechanically'



Real 2-body system
 (in the c.o.m. frame)

An effective particle of mass μ in some effective metric



$$\mu = \frac{m_1 m_2}{m_1 + m_2}$$



mass-shell constraint

$$0 = g_{\text{eff}}^{\mu\nu}(X) P_\mu P_\nu + \mu^2 + Q(X, P)$$

Level correspondence
 in the semi-classical limit:
Bohr-Sommerfeld \rightarrow
 identification of
 quantized action variables

$$J = \ell \hbar = \frac{1}{2\pi} \oint p_\varphi d\varphi$$

$$N = n \hbar = I_r + J$$

$$I_r = \frac{1}{2\pi} \oint p_r dr$$

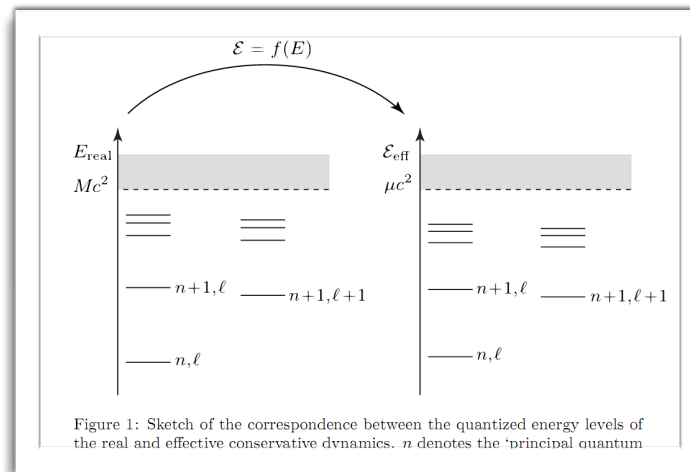


Figure 1: Sketch of the correspondence between the quantized energy levels of the real and effective conservative dynamics. n denotes the 'principal quantum'

Crucial energy map

$$\mathcal{E}_{\text{eff}} = \frac{(\mathcal{E}_{\text{real}})^2 - m_1^2 - m_2^2}{2(m_1 + m_2)}$$

as functions of I_r and $I_\phi = J$

New Angle of Attack on Two-Body Dynamics: Classical and/or Quantum Two-Body Scattering

TD 2016, 2017:

Gravitational scattering, post-Minkowskian approximation,
and effective-one-body theory

High-energy gravitational scattering and the general relativistic
two-body problem

A technique for translating the classical scattering function of two gravitationally interacting bodies into a corresponding (effective one-body) Hamiltonian description has been recently introduced [Phys. Rev. D **94**, 104015 (2016)]. Using this technique, we derive, for the first time, to second-order in Newton's constant (i.e. one classical loop) the Hamiltonian of two point masses having an arbitrary (possibly relativistic) relative velocity. The resulting (second post-Minkowskian) Hamiltonian is found to have a tame high-energy structure which we relate both to gravitational self-force studies of large mass-ratio binary systems, and to the ultra high-energy quantum scattering results of Amati, Ciafaloni and Veneziano. We derive several consequences of our second post-Minkowskian Hamiltonian: (i) the need to use special phase-space gauges to get a tame high-energy limit; and (ii) predictions about a (rest-mass independent) linear Regge trajectory behavior of high-angular-momenta, high-energy circular orbits. Ways of testing these predictions by dedicated numerical simulations are indicated. We finally indicate a way to connect our classical results to the quantum gravitational scattering amplitude of two particles, and we urge amplitude experts to use their novel techniques to compute the two-loop scattering amplitude of scalar masses, from which one could deduce the third post-Minkowskian effective one-body Hamiltonian.

one-loop
 G^2

two-loop
 G^3+G^4

Cheung-Rothstein-Solon 2018

From Scattering Amplitudes to Classical Potentials in the Post-Minkowskian Expansion

We combine tools from effective field theory and generalized unitarity to construct a map between on-shell scattering amplitudes and the classical potential for interacting spinless particles. For general relativity, we obtain analytic expressions for the classical potential of a binary black hole system at second order in the gravitational constant and all orders in velocity. Our results exactly match all known results up to fourth post-Newtonian order, and offer a simple check of future higher order calculations. By design, these methods should extend to higher orders in perturbation theory.

one-loop
 G^2

Simple Map: Conservative Scattering angle \leftrightarrow EOB dynamics

scattering angle, and its expansion in:

$$\frac{1}{j} = \frac{Gm_1 m_2}{J}$$

$$\frac{1}{2}\chi = \Phi(E_{\text{real}}, J; m_1, m_2, G)$$

TD'16-18
Bini-TD-Geralico'20

$$\frac{1}{2}\chi_{\text{class}}(E, J) = \frac{1}{j}\chi_1(\hat{E}_{\text{eff}}, \nu) + \frac{1}{j^2}\chi_2(\hat{E}_{\text{eff}}, \nu) + O(G^3)$$

$$0 = g_{\text{eff}}^{\mu\nu} P_\mu P_\nu + \mu^2 + Q$$

$$\chi_1(\hat{E}_{\text{eff}}, \nu) = \frac{2\hat{\mathcal{E}}_{\text{eff}}^2 - 1}{\sqrt{\hat{\mathcal{E}}_{\text{eff}}^2 - 1}}$$

$$\chi_2(\hat{E}_{\text{eff}}, \nu) = \frac{3\pi}{8} \frac{5\hat{\mathcal{E}}_{\text{eff}}^2 - 1}{\sqrt{1 + 2\nu(\hat{\mathcal{E}}_{\text{eff}} - 1)}}$$

Westpfahl'85

$$g_{\text{eff}}^{\mu\nu}$$

Schwarzschild
metric $M=m_1+m_2$

$$Q = \left(\frac{GM}{R}\right)^2 q_2(E) + \left(\frac{GM}{R}\right)^3 q_3(E) + O(G^4)$$

$$q_2(\hat{E}_{\text{eff}}, \nu) = -\frac{4}{\pi} [\chi_2(\hat{E}_{\text{eff}}, \nu) - \chi_2^{\text{Schw}}(\hat{E}_{\text{eff}})]$$

$$q_3(\hat{E}_{\text{eff}}, \nu) = \frac{4}{\pi} \frac{2\hat{\mathcal{E}}_{\text{eff}}^2 - 1}{\hat{\mathcal{E}}_{\text{eff}}^2 - 1} (\chi_2(\hat{E}_{\text{eff}}, \nu) - \chi_2^{\text{Schw}}(\hat{E}_{\text{eff}})) - \frac{\chi_3(\hat{E}_{\text{eff}}, \nu) - \chi_3^{\text{Schw}}(\hat{E}_{\text{eff}})}{\sqrt{\hat{\mathcal{E}}_{\text{eff}}^2 - 1}}$$

Linear combinations of the scattering coefficients!

$$\mathcal{E}_{\text{eff}} = \frac{(\mathcal{E}_{\text{real}})^2 - m_1^2 - m_2^2}{2(m_1 + m_2)}$$

$$\frac{\mathcal{E}_{\text{eff}}}{\mu} = \gamma = -\frac{p_1 \cdot p_2}{m_1 m_2}$$

$$q_2(\gamma, \nu) = \frac{3}{2}(5\gamma^2 - 1) \left(1 - \frac{1}{h(\gamma, \nu)}\right)$$

$$h(\gamma, \nu) = \sqrt{1 + 2\nu(\gamma - 1)}$$

Quantum Scattering Amplitudes and 2-body Dynamics

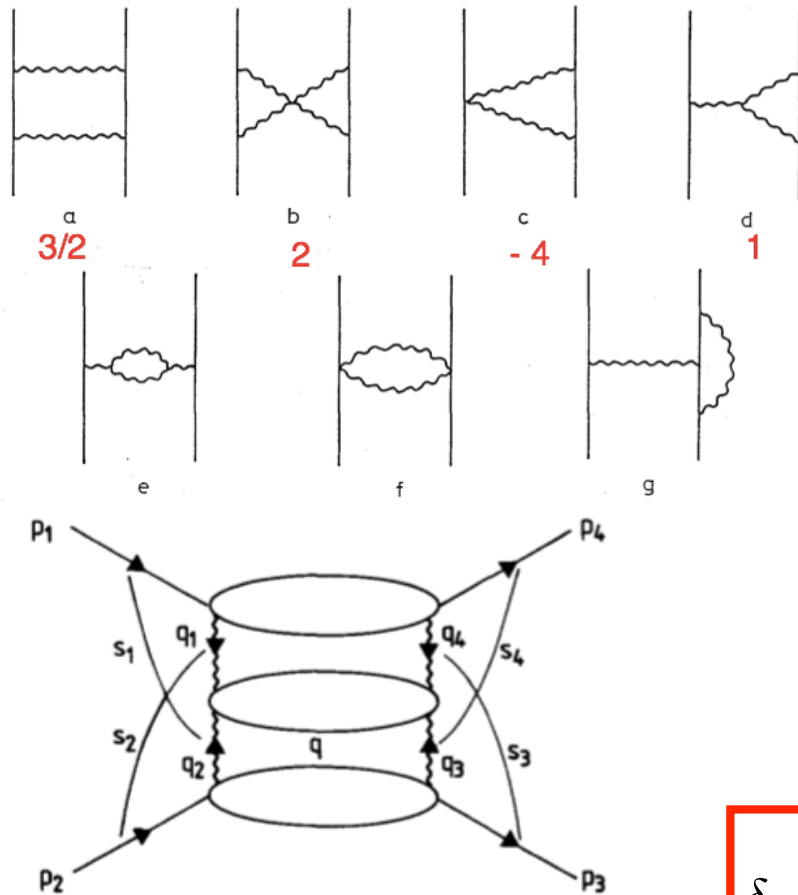


Fig. 3. The “H” diagram that provides the leading correction to the eikonal.

- Quantum Scattering Amplitudes → Potential one-graviton exchange :
Corinaldesi '56 '71,
Barker-Gupta-Haracz 66,
Barker-O'Connell 70, Hiida-Okamura72

Nonlinear: Iwasaki 71 [First post-Newtonian approx.],
Okamura-Ohta-Kimura-Hiida 73[2 PN]

Amati-Ciafaloni-Veneziano 1987-2008

Ultra-High-Energy ($s \gg M_{\text{Planck}}^2$)

Four-graviton Scattering at 2 loops

Eikonal phase δ in $D=4$
with one- and two-loop corrections
using the Regge-Gribov approach

confirmed by
DiVecchia+'19

$$\delta = \frac{Gs}{\hbar} \left(\log \left(\frac{L_{IR}}{b} \right) + \frac{6\ell_s^2}{\pi b^2} + \frac{2G^2 s}{b^2} \left(1 + \frac{2i}{\pi} \log(\dots) \right) \right)$$

Modern techniques for amplitudes (generalized unitarity; double copy; method of regions; IBPs; differential eqs; Bern, Dixon, Dunbar, Carrasco, Johansson, Cachazo et al., Bjerrum-Bohr et al., Cachazo-Guevara,...) can be used (Damour '17 CheungRothsteinSolon'18) to improve the classical 2-body dynamics: need a quantum/classical dictionary.

Application to the ACV eikonal scattering phase (massless or ultra-relativistic scattering)

Amati-Ciafaloni-Veneziano'90+ Ciafaloni-Colferai'14+ Bern et al'20+ DiVecchia et al'20

$$\delta^{\text{eikonal}} = \frac{1}{\hbar} (\delta^{\text{R}} + i\delta^{\text{I}}) + \text{quantum corr.}$$

$$\frac{1}{2} \chi^{\text{eikonal}} = 2 \frac{\gamma}{j} + \frac{16}{3} \frac{\gamma^3}{j^3} + \dots$$

**valid in the HE limit
gamma-> infty**

Using the $\chi \rightarrow Q$ dictionary
this corresponds to the HE limits:

$$q_2^{\text{HE}} = \frac{15}{2} \gamma^2$$

$$q_3^{\text{HE}} = \gamma^2$$

i.e. an HE limit for the EOB mass-shell condition (TD'18)

$$0 = g_{\text{eff}}^{\mu\nu}(X) P_\mu P_\nu + \mu^2 + Q(X, P)$$

$$0 = g_{\text{Schw}}^{\mu\nu} P_\mu P_\nu + \left(\frac{15}{2} \left(\frac{GM}{R} \right)^2 + \left(\frac{GM}{R} \right)^3 \right) P_0^2$$

Translating quantum scattering amplitudes into classical dynamical information (1)

The domain of validity of the Born-Feynman expansion

$$\mathcal{M}(s, t) = \mathcal{M}^{(\frac{G}{\hbar})}(s, t) + \mathcal{M}^{(\frac{G^2}{\hbar^2})}(s, t) + \dots, \quad \mathcal{M}^{(\frac{G}{\hbar})}(s, t) = 16\pi \frac{G}{\hbar} \frac{2(p_1 \cdot p_2)^2 - p_1^2 p_2^2}{-t}.$$

is

$$\frac{Gs}{\hbar v} \sim \frac{GE_1 E_2}{\hbar v} \ll 1$$

while the domain of validity of classical scattering is (Bohr 1948)

$$\frac{Gs}{\hbar v} \sim \frac{GE_1 E_2}{\hbar v} \gg 1$$

Amati-Ciafaloni-Veneziano faced this issue by assuming **eikonalization in b space**

$$\tilde{\mathcal{A}}(s, b) = \int \frac{d^{D-2}q}{(2\pi)^{D-2}} \frac{\mathcal{A}(s, q^2)}{4pE} e^{-ib \cdot q}$$

$$1 + i\tilde{\mathcal{A}}(s, b) = (1 + 2i\Delta(s, b)) e^{2i\delta(s, b)}$$

classical phase

$$i \frac{\mathcal{A}(s, Q^2)}{4pE} = \int d^{D-2}b \left(e^{2i\delta(s, b)} - 1 \right) e^{ib \cdot Q}$$

$$2\delta(s, b) = \frac{\Delta S_r(s, J)}{\hbar}$$

total classical momentum transfer:

$$Q^\mu = - \frac{\partial \text{Re } 2\delta(s, b)}{\partial b^\mu}$$

subtracted radial action of potential scattering

Translating quantum scattering amplitudes into classical dynamical information (2)

Damour'17: EOB potential $Q(R,E)$ or $W(R,E)$

Cheung-Rothstein-Solon'18, Bern et al'19

different EFT potential $V(R,P^2)$ and methods for

taking the classical limit at the integrand level,

and extracting the « classical part » of the scattering amplitude

EOB

$$Q^E(u, \mathcal{E}_{\text{eff}}) = u^2 q_2(\mathcal{E}_{\text{eff}}) + u^3 q_3(\mathcal{E}_{\text{eff}}) + u^4 q_4^E(\mathcal{E}_{\text{eff}}) + O(G^5)$$

$$w(r, p_\infty) = \frac{w_1(\gamma)}{r} + \frac{w_2(\gamma)}{r^2} + \frac{w_3(\gamma)}{r^3} + \frac{w_4(\gamma)}{r^4} + \dots$$

EFT

$$H(\mathbf{P}, \mathbf{X}) = \sqrt{m_1^2 + \mathbf{P}^2} + \sqrt{m_2^2 + \mathbf{P}^2} + V(R, \mathbf{P}^2)$$

$$V(R, \mathbf{P}^2) = G \frac{c_1(\mathbf{P}^2)}{R} + G^2 \frac{c_2(\mathbf{P}^2)}{R^2} + G^3 \frac{c_3(\mathbf{P}^2)}{R^3} + \dots$$

non-relativistic potential scattering !

$$-\hat{\hbar}^2 \Delta_{\mathbf{x}} \psi(\mathbf{x}) = \left[p_\infty^2 + \frac{w_1}{r} + \frac{w_2}{r^2} + \frac{w_3}{r^3} + O\left(\frac{1}{r^4}\right) \right] \psi(\mathbf{x})$$

$$\mathcal{M}_{\text{classical}}^{QFT} = \frac{8\pi G s}{\hbar} f^{EOB} = \mathcal{M}^{EFT}$$

Scattering Amplitudes and the Conservative Hamiltonian for Binary Systems at Third Post-Minkowskian Order

Zvi Bern,¹ Clifford Cheung,² Radu Roiban,³ Chia-Hsien Shen,¹ Mikhail P. Solon,² and Mao Zeng⁴

¹Mani L. Bhaumik Institute for Theoretical Physics, University of California at Los Angeles, Los Angeles, California 90095, USA

²Walter Burke Institute for Theoretical Physics, California Institute of Technology, Pasadena, California 91125

³Institute for Gravitation and the Cosmos, Pennsylvania State University, University Park, Pennsylvania 16802, USA

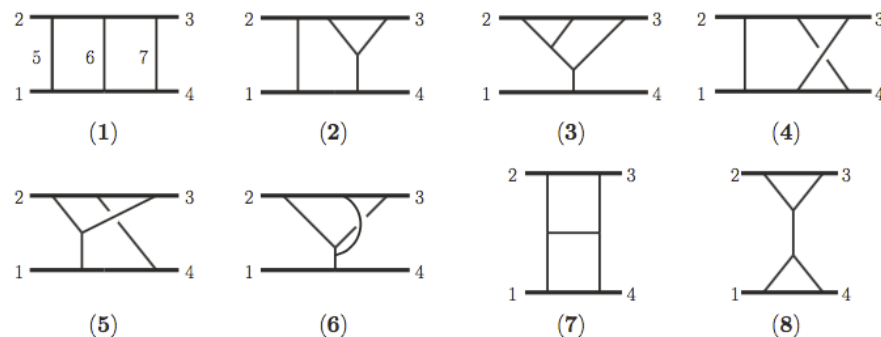
⁴Institute for Theoretical Physics, ETH Zürich, 8093 Zürich, Switzerland

 (Received 28 January 2019; published 24 May 2019)

two-loop
level
 G^3

We present the amplitude for classical scattering of gravitationally interacting massive scalars at third post-Minkowskian order. Our approach harnesses powerful tools from the modern amplitudes program such as generalized unitarity and the double-copy construction, which relates gravity integrands to simpler gauge-theory expressions. Adapting methods for integration and matching from effective field theory, we extract the conservative Hamiltonian for compact spinless binaries at third post-Minkowskian order. The resulting Hamiltonian is in complete agreement with corresponding terms in state-of-the-art expressions at fourth post-Newtonian order as well as the probe limit at all orders in velocity. We also derive the scattering angle at third post-Minkowskian order and find agreement with known results.

the eight
2-loop diagrams
contributing
to the $O(G^3/r^3)$
classical potential



two-loop level

$$\mathcal{M}_3 = \frac{\pi G^3 \nu^2 m^4 \log q^2}{6\gamma^2 \xi} \left[3 - 6\nu + 206\nu\sigma - 54\sigma^2 + 108\nu\sigma^2 + 4\nu\sigma^3 - \frac{48\nu(3 + 12\sigma^2 - 4\sigma^4) \operatorname{arcsinh} \sqrt{\frac{\sigma-1}{2}}}{\sqrt{\sigma^2 - 1}} - \frac{18\nu\gamma(1 - 2\sigma^2)(1 - 5\sigma^2)}{(1 + \gamma)(1 + \sigma)} \right] + \frac{8\pi^3 G^3 \nu^4 m^6}{\gamma^4 \xi} [3\gamma(1 - 2\sigma^2)(1 - 5\sigma^2)F_1 - 32m^2\nu^2(1 - 2\sigma^2)^3 F_2], \quad (8)$$

 arcsinh

3PM computation (Bern-Cheung-Roiban-Shen-Solon-Zeng'19)

using a combination of techniques: generalized unitarity; BCJ double-copy; 2-loop amplitude of quasi-classical diagrams; **EFT transcription** (Cheung-Rothstein-Solon'18);
resummation of PN-expanded integrals for potential-gravitons

$$\chi_3^{\text{cons}} = \chi_3^{\text{Schw}} - \frac{2\nu\sqrt{\gamma^2 - 1}}{h^2(\gamma, \nu)} \bar{C}^{\text{cons}}(\gamma) \quad \text{G}^3 \text{ contrib. to H_EOB}$$

$$q_3^{\text{cons}} = \frac{3}{2} \frac{(2\gamma^2 - 1)(5\gamma^2 - 1)}{\gamma^2 - 1} \left(\frac{1}{h(\gamma, \nu)} - 1 \right) + \frac{2\nu}{h^2(\gamma, \nu)} \bar{C}^{\text{cons}}(\gamma)$$

$$\bar{C}^{\text{cons}}(\gamma) = \frac{2}{3}\gamma(14\gamma^2 + 25) + 2(4\gamma^4 - 12\gamma^2 - 3) \frac{\mathcal{A}(v)}{\sqrt{\gamma^2 - 1}}$$

$$h(\gamma, \nu) \equiv \frac{\sqrt{s}}{\lambda r} = \sqrt{1 + 2\nu(\gamma - 1)}$$

$$\mathcal{A}(v) \equiv \text{arctanh}(v) = \frac{1}{2} \ln \frac{1+v}{1-v} = 2 \text{arcsinh} \sqrt{\frac{\gamma - 1}{2}}$$

puzzling HE limits when compared to ACV and Akcay et al'12

$$\frac{1}{2} \chi^{\text{cons}} = 2 \frac{\gamma}{j} + (12 - 8 \ln(2\gamma)) \frac{\gamma^3}{j^3} + O(G^4)$$

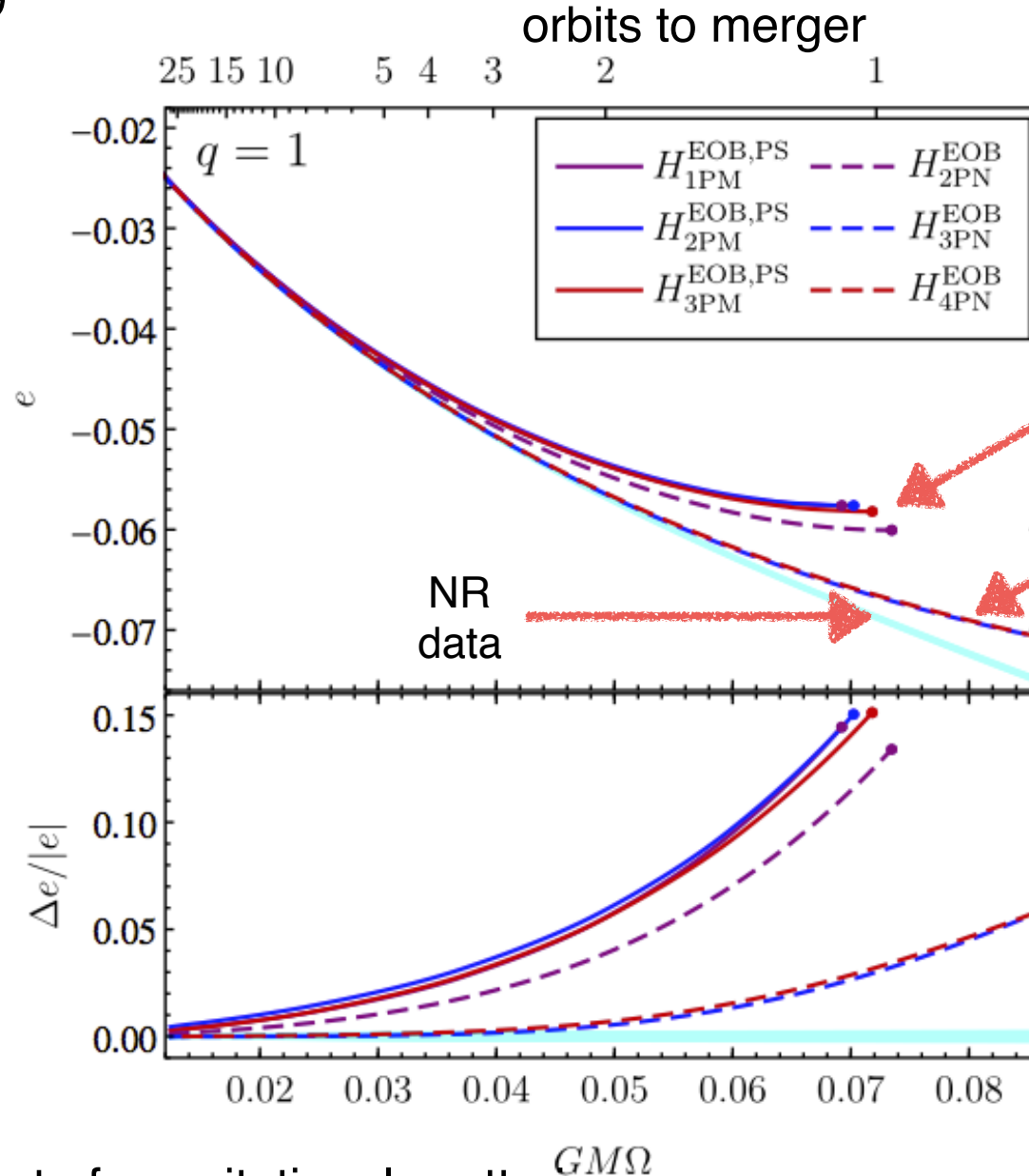
$$q_3^{\text{cons}} \approx +8 \ln(2\gamma) \gamma^2 \quad \text{instead of} \quad q_3^{\text{ACV}} \approx +1 \gamma^2$$

confirmations: 5PN (Bini-TD-Geralico'19); 6PN (Blümlein-Maier-Marquard-Schäfer'20, Bini-TD-Geralico'20); 3PM (Cheung-Solon'20, Kälin-Porto'20)

Comparison of 3PM Hamiltonian to NR energetics

Antonelli et al. '19

fractional binding energy versus angular frequency



PM Hamiltonians up to G^3

PN Hamiltonians used in LIGO-Virgo data-analysis

includes terms $O(G^5)$ and resummation

The main current interest of gravitational scattering results is **conceptual**, rather than directly practical

Conservative and Radiative Aspects of the Dynamics

selected
by Bern's
integration
method
of regions

2PM

1PM

$$\dot{p}_a \sim G \left(1 + \frac{1}{c^2} + \frac{1}{c^4} + \frac{1}{c^6} + \frac{1}{c^8} + \frac{1}{c^{10}} \right) +$$

$$+ G^2 \left(\frac{1}{c^2} + \frac{1}{c^4} + \frac{1}{c^5} + \frac{1}{c^6} + \frac{1}{c^7} + \frac{1}{c^8} + \frac{1}{c^9} + \frac{1}{c^{10}} \right) +$$

$$+ G^3 \left(\frac{1}{c^4} + \frac{1}{c^5} + \frac{1}{c^6} + \frac{1}{c^7} + \frac{1}{c^8} + \frac{1}{c^9} + \frac{1}{c^{10}} \right) +$$

1PN

$$+ G^4 \left(\frac{1}{c^6} + \frac{1}{c^7} + \frac{1}{c^8} + \frac{1}{c^9} + \frac{1}{c^{10}} \right) +$$

2PN

2.5PN

LO

rad reac

$$+ G^5 \left(\frac{1}{c^8} + \frac{1}{c^9} + \frac{1}{c^{10}} \right) +$$

$$+ G^6 \frac{1}{c^{10}}$$

Black: time-even and conservative

Red: time-odd and dissipative

Blue: nonlocal-in-time but decomposable
in conservative and dissipative

Purple: ambiguous in various ways ??

4PN

(G⁴, G⁵)

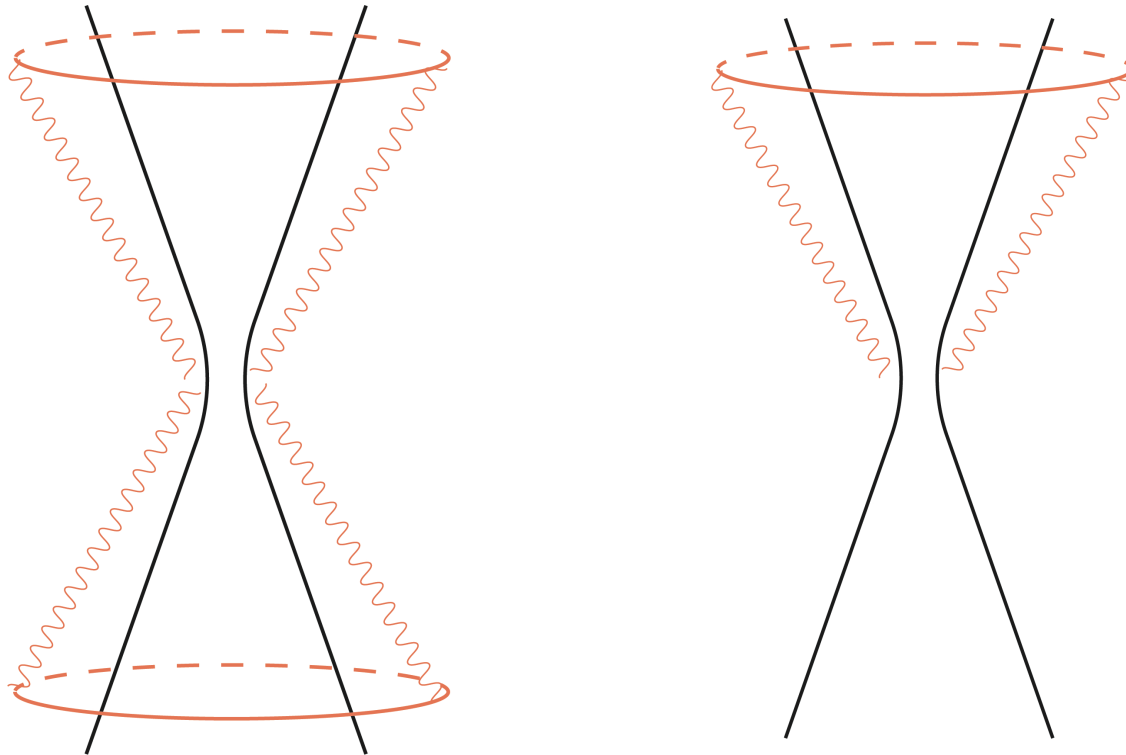
separation
well-defined



5PN

same order as
F_radreac²!

Conservative vs Radiation-reacted Classical Gravitational Scattering



Radiation-reaction effects enter scattering at G^3/c^5 (Bini-TD'12)

$$\frac{1}{2}\chi^{\text{rad}} = + \frac{8G^3}{5c^5} \frac{m_1^3 m_2^3}{J^3} \nu v^2 + \dots$$

Radiation-reaction effects in scattering play a crucial role at **high-energy**

(DiVecchia-Heissenberg-Russo-Veneziano'20, TD'21, Hermann-Parra-Martinez-Ruf-Zeng'21,....)

they resolve the puzzle of the discrepancy between the HE limit of

Amati-Ciafaloni-Veneziano'90(+ Ciafaloni-Colferai'14), and the G^3 result of Bern et al'19,20₂₀

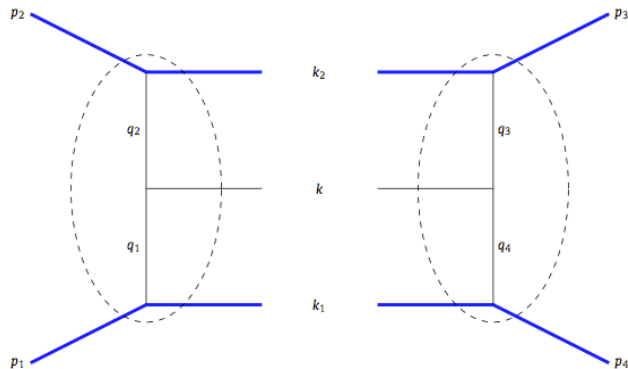
Universality of ultra-relativistic gravitational scattering from analyticity/crossing (DiVecchia-Heissenberg-Russo-Veneziano'20)

ultra-relativistic eikonal phase: $\delta(s, b) = \delta_0(s, b) + \delta_2(s, b)$

$$\text{Re}(2\delta_2) = \frac{\pi}{2 \log s} \text{Im}(2\delta_2) - \frac{\delta_0}{s} (\nabla 2\delta_0)^2 + \mathcal{O}\left(\frac{1}{\log s}\right)$$

IR
finite

IR
divergent



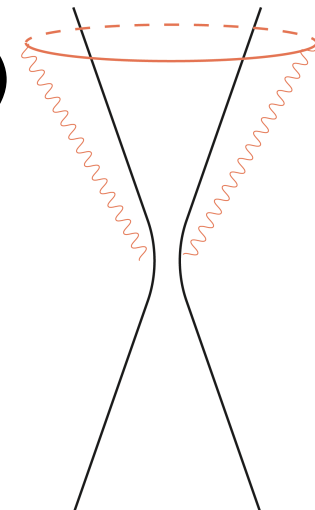
$$\text{Im} \widetilde{A}_2^{(3p)}(s, b) \simeq \frac{1}{2s} \frac{(8G_N s)^3 \log s \Gamma^3(1-\epsilon)}{16(\pi b^2)^{1-3\epsilon}} \left[-\frac{1}{4\epsilon} + \frac{1}{2} + \mathcal{O}(\epsilon) \right]$$

$$\text{Re}(2\delta_2) \simeq \frac{4G_N^3 s^2}{\hbar b^2}$$

universality of HE result = ACV, thanks to radiative effects

✦ DiVecchia-Heissenberg-Russo-Veneziano'21: **Radiation Reaction from Soft Theorems**

Radiation-Reaction Contribution to the (transverse) Classical Scattering Angle at G^3 (TD 2010.01641)



$$\chi^{\text{tot}} = \chi^{\text{cons}} + \chi^{\text{rad}}$$

where, to first order in Rad-Reac, one has (Bini-TD'12)

$$\chi^{\text{rad}}(E, J) = -\frac{1}{2} \frac{\partial \chi^{\text{cons}}}{\partial E} E^{\text{rad}} - \frac{1}{2} \frac{\partial \chi^{\text{cons}}}{\partial J} J^{\text{rad}}$$

$O(G^2)$

[TD-Deruelle'81]

$$h_{ij}^{\text{TT}} = \frac{f_{ij}(t-r, \theta, \phi)}{r} + O\left(\frac{1}{r^2}\right)$$

$$J_k^{\text{rad}} = \frac{\epsilon_{kij}}{16\pi G} \int du d\Omega \left[f_{ia} \partial_u f_{ja} - \frac{1}{2} x^i \partial_j f_{ab} \partial_u f_{ab} \right]$$

DeWitt'71, Thorne'80

Kovacs-Thorne'77, Bel et al'81,

Westpfahl'85

$\chi^{\text{cons}} = O(G^1)$

$O(G^3)$

$O(G^4)$

$O(G^3)$

$$\mathcal{I}(v) = -\frac{16}{3} + \frac{2}{v^2} + \frac{2(3v^2 - 1)}{v^3} \mathcal{A}(v) \quad \mathcal{A}(v) \equiv \text{arctanh}(v) = \frac{1}{2} \ln \frac{1+v}{1-v}$$

$$\frac{1}{2} \chi^{\text{rad}}(\gamma, j, \nu) = + \frac{\nu}{h^2(\gamma, \nu) j^3} (2\gamma^2 - 1)^2 \mathcal{I}(v) + O(G^4)$$

$$\frac{1}{2} (\chi^{\text{cons}} + \chi^{\text{rad}}) = 2 \frac{\gamma}{j} + \frac{16}{3} \frac{\gamma^3}{j^3} = \chi^{\text{ACV}}$$

Translating quantum scattering amplitudes into classical dynamical information (3)

Kosower-Maybe-O'Connell'19 formalism for any observable O

$$\Delta O = \langle \text{out} | O | \text{out} \rangle - \langle \text{in} | O | \text{in} \rangle \quad \text{with } |\text{out}\rangle = S |\text{in}\rangle \text{ and } S = 1 + iT$$

$$\Delta O = \langle \text{in} | i[O, T] | \text{in} \rangle + \langle \text{in} | T^\dagger [O, T] | \text{in} \rangle$$

Hermann-Parra-Martinez-Ruf-Zeng'21 making use of: generalized unitarity, reverse unitarity (for phase-space integrals), method of regions, integration by parts canonical differential eqs applied KMOC to $O = p_{-1}^\mu$ and p_{rad}^μ

$$\begin{aligned} \mathcal{I}_\perp^{(2)} = & \text{Diagram} - i \int d\tilde{\Phi}_2 \frac{\ell_1 \cdot q}{q^2} \left[\text{Diagram 1} + \text{Diagram 2} \right] \\ & - i \int d\tilde{\Phi}_3 \frac{\ell_1 \cdot q}{q^2} \text{Diagram 3} \end{aligned} \quad (6.14)$$

momentum transfer (impulse)

(Hermann-Parra-Martinez-Ruf-Zeng'21)

$$\Delta p_{1,\perp,\text{cons}}^{\mu,(2)} = \frac{G^3 M^4 \nu}{|b|^3} \frac{2}{\sqrt{\sigma^2-1}} \frac{b^\mu}{|b|} \left[h^2(\sigma, \nu) \left(16\sigma^2 - \frac{1}{(\sigma^2-1)^2} \right) - \frac{4}{3} \nu \sigma (14\sigma^2 + 25) - 8\nu (4\sigma^4 - 12\sigma^2 - 3) \frac{\text{arcsinh} \sqrt{\frac{\sigma-1}{2}}}{\sqrt{\sigma^2-1}} \right] \quad (7)$$

$$\Delta p_{1,u,\text{cons}}^{\mu,(2)} = \frac{G^3 M^5 \nu^2}{|b|^3} \frac{3\pi (2\sigma^2-1) (5\sigma^2-1)}{2(\sigma^2-1)} \left[\frac{1}{m_1} \check{u}_1^\mu - \frac{1}{m_2} \check{u}_2^\mu \right]$$

$$\Delta p_{1,\text{rad}}^{\mu,(2)} = \frac{G^3 M^4 \nu^2}{|b|^3} \left\{ \frac{4}{\sqrt{\sigma^2-1}} \frac{b^\mu}{|b|} \left[f_1^{\text{LS}}(\sigma) + f_3^{\text{LS}}(\sigma) \frac{\sigma \text{arcsinh} \sqrt{\frac{\sigma-1}{2}}}{\sqrt{\sigma^2-1}} \right] + \pi \check{u}_2^\mu \left[f_1(\sigma) + f_2(\sigma) \log \left(\frac{\sigma+1}{2} \right) + f_3(\sigma) \frac{\sigma \text{arcsinh} \sqrt{\frac{\sigma-1}{2}}}{\sqrt{\sigma^2-1}} \right] \right\}.$$

$$f_1^{\text{LS}}(\sigma) = -\frac{(2\sigma^2-1)^2(5\sigma^2-8)}{3(\sigma^2-1)^{3/2}},$$

$$f_3^{\text{LS}}(\sigma) = \frac{2(2\sigma^2-1)^2(2\sigma^2-3)}{(\sigma^2-1)^{3/2}},$$

$$f_1(\sigma) = \frac{210\sigma^6 - 552\sigma^5 + 339\sigma^4 - 912\sigma^3 + 3148\sigma^2 - 3336\sigma + 1151}{48(\sigma^2-1)^{3/2}},$$

$$f_2(\sigma) = -\frac{35\sigma^4 + 60\sigma^3 - 150\sigma^2 + 76\sigma - 5}{8\sqrt{\sigma^2-1}},$$

$$f_3(\sigma) = \frac{(2\sigma^2-3)(35\sigma^4-30\sigma^2+11)}{8(\sigma^2-1)^{3/2}}.$$

radiated 4-momentum

$$\Delta R^\mu = \frac{G^3 m_1^2 m_2^2}{|b|^3} \frac{u_1^\mu + u_2^\mu}{\sigma+1} \mathcal{E}(\sigma) + \mathcal{O}(G^4)$$

$$\frac{\mathcal{E}(\sigma)}{\pi} = f_1(\sigma) + f_2(\sigma) \log \left(\frac{\sigma+1}{2} \right) + f_3(\sigma) \frac{\sigma \text{arcsinh} \sqrt{\frac{\sigma-1}{2}}}{\sqrt{\sigma^2-1}}$$

High-energy puzzle

$$\mathcal{E}(\gamma) \propto \gamma^3$$

see also: DiVecchia et al, Riva-Vernizzi'21, Bjerrum-Bohr-Plante-Vanhove-Damgaard, useful results concerning the **waveform** (using QFT integration methods)...

potential gravitons only

Scattering Amplitudes and Conservative Binary Dynamics at $\mathcal{O}(G^4)$

Zvi Bern,¹ Julio Parra-Martinez¹,² Radu Roiban,³ Michael S. Ruf¹,⁴

Chia-Hsien Shen⁵, Mikhail P. Solon,¹ and Mao Zeng⁶

¹*Mani I. Bhaumik Institute for Theoretical Physics University of California at Los Angeles*

three-loop
level
 G^4

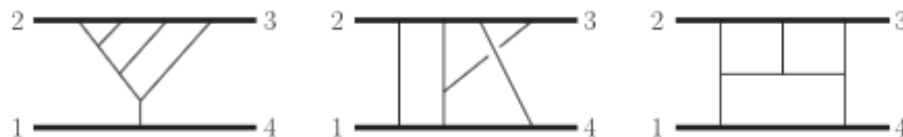


FIG. 2. Sample diagrams at $\mathcal{O}(G^4)$. From left to right: a contribution in the probe limit, a nonplanar diagram that contains iteration terms, and a diagram that contains contributions related to the tail effect.

IR-divergent
because
lacks tail effects

$$\begin{aligned}
 \mathcal{M}_4(\mathbf{q}) &= G^4 M^7 \nu^2 |\mathbf{q}| \left(\frac{\mathbf{q}^2}{4^{1/3} \tilde{\mu}^2} \right)^{-3\epsilon} \pi^2 \left[\mathcal{M}_4^p + \nu \left(\frac{\mathcal{M}_4^t}{\epsilon} + \mathcal{M}_4^f \right) \right] + \int_{\epsilon} \frac{\tilde{I}_{r,1}^4}{Z_1 Z_2 Z_3} + \int_{\epsilon} \frac{\tilde{I}_{r,1}^2 \tilde{I}_{r,2}}{Z_1 Z_2} + \int_{\epsilon} \frac{\tilde{I}_{r,1} \tilde{I}_{r,3}}{Z_1} + \int_{\epsilon} \frac{\tilde{I}_{r,2}^2}{Z_1}, \\
 \mathcal{M}_4^p &= -\frac{35(1-18\sigma^2+33\sigma^4)}{8(\sigma^2-1)}, \quad \mathcal{M}_4^t = h_1 + h_2 \log\left(\frac{\sigma+1}{2}\right) + h_3 \frac{\text{arccosh}(\sigma)}{\sqrt{\sigma^2-1}}, \\
 \mathcal{M}_4^f &= h_4 + h_5 \log\left(\frac{\sigma+1}{2}\right) + h_6 \frac{\text{arccosh}(\sigma)}{\sqrt{\sigma^2-1}} + h_7 \log(\sigma) - h_2 \frac{2\pi^2}{3} + h_8 \frac{\text{arccosh}^2(\sigma)}{\sigma^2-1} + h_9 \left[\text{Li}_2\left(\frac{1-\sigma}{2}\right) + \frac{1}{2} \log^2\left(\frac{\sigma+1}{2}\right) \right] \\
 &\quad + h_{10} \left[\text{Li}_2\left(\frac{1-\sigma}{2}\right) - \frac{\pi^2}{6} \right] + h_{11} \left[\text{Li}_2\left(\frac{1-\sigma}{1+\sigma}\right) - \text{Li}_2\left(\frac{\sigma-1}{\sigma+1}\right) + \frac{\pi^2}{3} \right] + h_2 \frac{2\sigma(2\sigma^2-3)}{(\sigma^2-1)^{3/2}} \left[\text{Li}_2\left(\sqrt{\frac{\sigma-1}{\sigma+1}}\right) - \text{Li}_2\left(-\sqrt{\frac{\sigma-1}{\sigma+1}}\right) \right] \\
 &\quad + \frac{2h_3}{\sqrt{\sigma^2-1}} \left[\text{Li}_2(1-\sigma-\sqrt{\sigma^2-1}) - \text{Li}_2(1-\sigma+\sqrt{\sigma^2-1}) + 5\text{Li}_2\left(\sqrt{\frac{\sigma-1}{\sigma+1}}\right) - 5\text{Li}_2\left(-\sqrt{\frac{\sigma-1}{\sigma+1}}\right) \right] \\
 &\quad + 2\log\left(\frac{\sigma+1}{2}\right) \text{arccosh}(\sigma) \left. \right] + h_{12} K^2\left(\frac{\sigma-1}{\sigma+1}\right) + h_{13} K\left(\frac{\sigma-1}{\sigma+1}\right) E\left(\frac{\sigma-1}{\sigma+1}\right) + h_{14} E^2\left(\frac{\sigma-1}{\sigma+1}\right), \tag{6}
 \end{aligned}$$

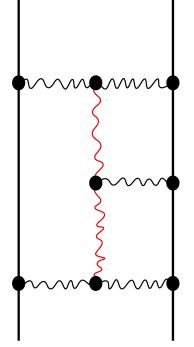
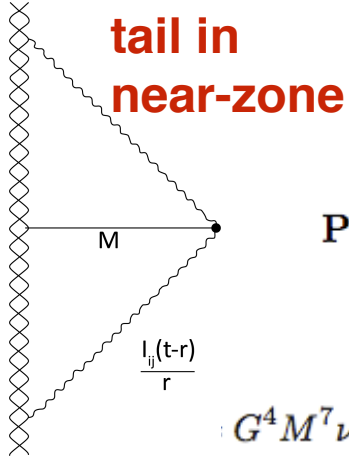
soft (radiationlike) gravitons

Scattering Amplitudes, the Tail Effect, and Conservative Binary Dynamics at $\mathcal{O}(G^4)$

Zvi Bern,¹ Julio Parra-Martinez,² Radu Roiban,³ Michael S. Ruf,¹
Chia-Hsien Shen,⁴ Mikhail P. Solon,¹ and Mao Zeng⁵

Conservative Dynamics of Binary Systems at Fourth Post-Minkowskian Order in the Large-eccentricity Expansion

Christoph Dlapa,¹ Gregor Kälin,¹ Zhengwen Liu,¹ and Rafael A. Porto¹



$$G^4 M^7 \nu^2 |\mathbf{q}| \pi^2 \left[\mathcal{M}_4^{\text{P}} + \nu \left(4\mathcal{M}_4^{\text{t}} \log\left(\frac{p_\infty}{2}\right) + \mathcal{M}_4^{\pi^2} + \mathcal{M}_4^{\text{rem}} \right) \right] + \int_{\ell} \frac{\tilde{I}_{r,1}^4}{Z_1 Z_2 Z_3} + \int_{\ell} \frac{\tilde{I}_{r,1}^2 \tilde{I}_{r,2}}{Z_1 Z_2} + \int_{\ell} \frac{\tilde{I}_{r,1} \tilde{I}_{r,3}}{Z_1} + \int_{\ell} \frac{\tilde{I}_{r,2}^2}{Z_1},$$

$$\mathcal{M}_4^{\text{P}} = -\frac{35(1 - 18\sigma^2 + 33\sigma^4)}{8(\sigma^2 - 1)},$$

$$\mathcal{M}_4^{\text{t}} = r_1 + r_2 \log\left(\frac{\sigma+1}{2}\right) + r_3 \frac{\text{arccosh}(\sigma)}{\sqrt{\sigma^2 - 1}}, \quad (3)$$

$$\mathcal{M}_4^{\pi^2} = r_4 \pi^2 + r_5 K\left(\frac{\sigma-1}{\sigma+1}\right) E\left(\frac{\sigma-1}{\sigma+1}\right) + r_6 K^2\left(\frac{\sigma-1}{\sigma+1}\right) + r_7 E^2\left(\frac{\sigma-1}{\sigma+1}\right),$$

$$\mathcal{M}_4^{\text{rem}} = r_8 + r_9 \log\left(\frac{\sigma+1}{2}\right) + r_{10} \frac{\text{arccosh}(\sigma)}{\sqrt{\sigma^2 - 1}} + r_{11} \log(\sigma) + r_{12} \log^2\left(\frac{\sigma+1}{2}\right) + r_{13} \frac{\text{arccosh}(\sigma)}{\sqrt{\sigma^2 - 1}} \log\left(\frac{\sigma+1}{2}\right) + r_{14} \frac{\text{arccosh}^2(\sigma)}{\sigma^2 - 1} \\ + r_{15} \text{Li}_2\left(\frac{1-\sigma}{2}\right) + r_{16} \text{Li}_2\left(\frac{1-\sigma}{1+\sigma}\right) + r_{17} \frac{1}{\sqrt{\sigma^2 - 1}} \left[\text{Li}_2\left(-\sqrt{\frac{\sigma-1}{\sigma+1}}\right) - \text{Li}_2\left(\sqrt{\frac{\sigma-1}{\sigma+1}}\right) \right].$$

$$\mathcal{M}_4^{\text{radgrav,f}} = \frac{12044}{75} p_\infty^2 + \frac{212077}{3675} p_\infty^4 + \frac{115917979}{793800} p_\infty^6 \\ - \frac{9823091209}{76839840} p_\infty^8 + \frac{115240251793703}{1038874636800} p_\infty^{10} \\ - \frac{411188753665637}{4155498547200} p_\infty^{12} + \dots, \quad (6)$$

**matches the 6PN
result of the
Tutti Frutti approach
(Bini-D-Geralico'21)**

whose first three terms match the sixth PN order result in Eq. (6.20) of Ref. [42].

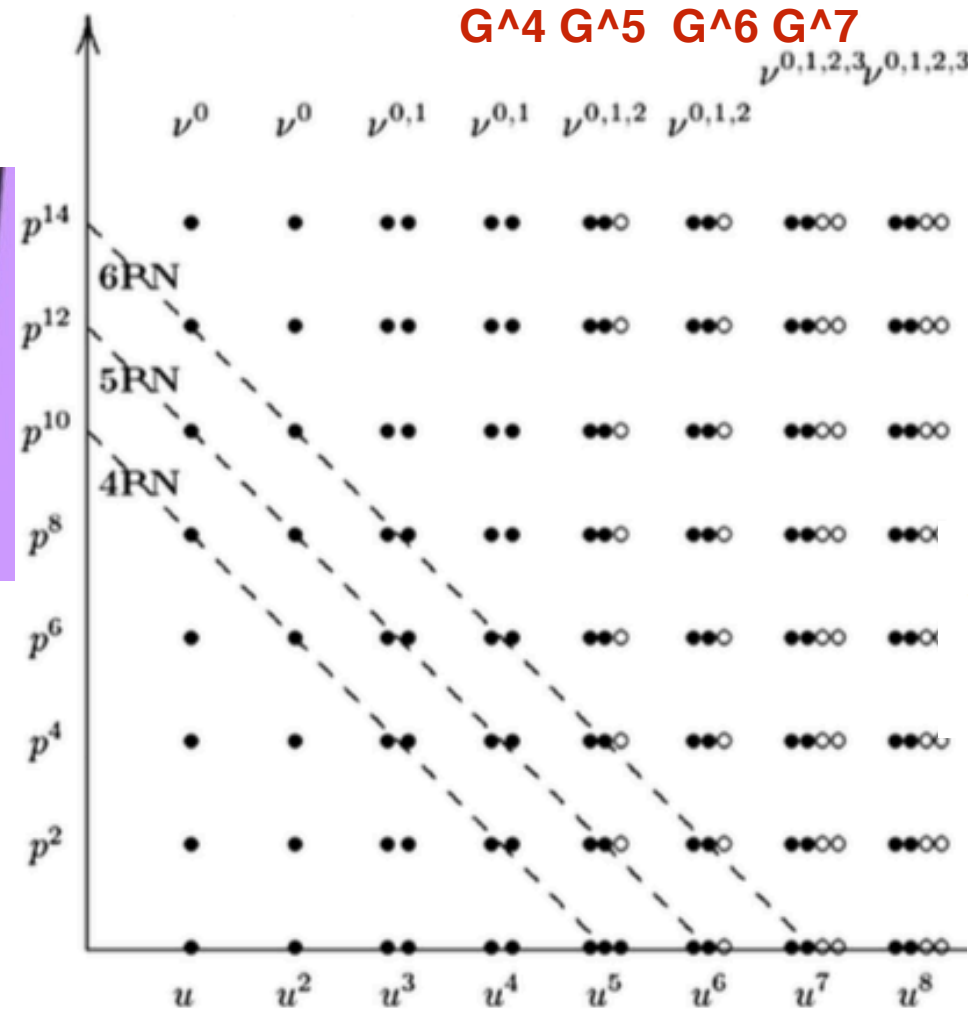
Tutti-Frutti method



(Bini-TD-Geralico '19,'20'21)

combines
PN
MPM
EOB

Delaunay
Self-Force
Scattering
properties



6PN
conservative
dynamics
complete at
3PM and 4PM

$$S_{\text{nonloc}}^{4+5\text{PN}}[x_1(s_1), x_2(s_2)] = \frac{G^2 \mathcal{M}}{c^3} \int dt \text{PF}_{2r_{12}^h(t)/c} \times \int \frac{dt'}{|t-t'|} \mathcal{F}_{\text{IPN}}^{\text{split}}(t, t')$$

$$\mathcal{F}_{\text{IPN}}^{\text{split}}(t, t') = \frac{G}{c^5} \left(\frac{1}{5} I_{ab}^{(3)}(t) I_{ab}^{(3)}(t') + \frac{1}{189c^2} + \frac{16}{45c^2} J_{ab}^{(3)}(t) J_{ab}^{(3)}(t') \right)$$

FIG. 1. Schematic representation of the irreducible information contained, at each post-Minkowskian level (keyed by a power of $u = GM/r$), in the local dynamics. Each vertical column of dots describes the post-Newtonian expansion (keyed by powers of p^2) of an energy-dependent function parametrizing the scattering angle. The various columns at a given post-Minkowskian level correspond to increasing powers of the symmetric mass-ratio ν . See text for details.

Classical scattering perturbation theory enhanced by using QFT integration methods

$$\frac{dx_a^\mu}{d\sigma_a} = g^{\mu\nu}(x_a) p_{a\nu},$$

$$\frac{dp_{a\mu}}{d\sigma_a} = -\frac{1}{2} \partial_\mu g^{\alpha\beta}(x_a) p_{a\alpha} p_{a\beta}.$$

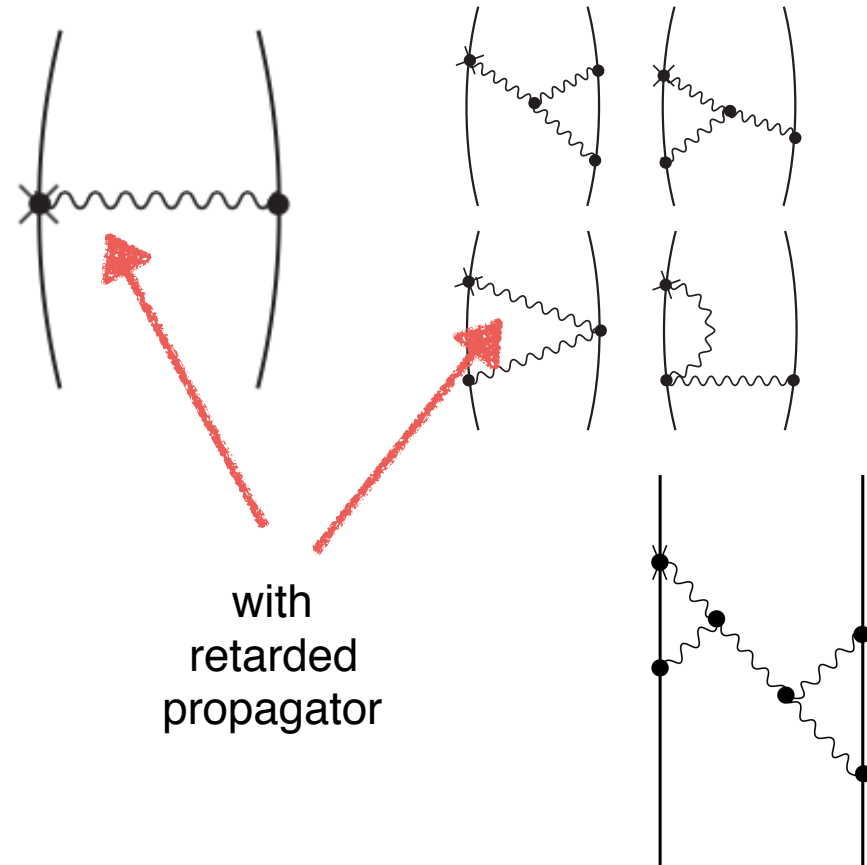
$$R^{\mu\nu} - \frac{1}{2} R g^{\mu\nu} = 8\pi G T^{\mu\nu}$$

$$T^{\mu\nu}(x) = \sum_a \int d\sigma_a p_a^\mu p_a^\nu \frac{\delta^4(x - x_a(\sigma_a))}{\sqrt{g}}$$

$$\begin{aligned} \Delta p_{a\mu} &= \int_{-\infty}^{+\infty} d\sigma_a \frac{dp_{a\mu}}{d\sigma_a} \\ &= -\frac{1}{2} \int_{-\infty}^{+\infty} d\sigma_a \partial_\mu g^{\alpha\beta}(x_a) p_{a\alpha} p_{a\beta}. \end{aligned}$$

$$\begin{aligned} \Delta p_{1\mu} &= 2G \int d\sigma_1 d\sigma_2 p_{1\alpha} p_{1\beta} \\ &\quad \times \partial_\mu \mathcal{P}^{\alpha\beta;\alpha'\beta'}(x_1(\sigma_1) - x_2(\sigma_2)) p_{2\alpha'} p_{2\beta'} \end{aligned}$$

$$\mathcal{P}^{\alpha\beta;\alpha'\beta'}(x - y) = \left(\eta^{\alpha\alpha'} \eta^{\beta\beta'} - \frac{1}{2} \eta^{\alpha\beta} \eta^{\alpha'\beta'} \right) \mathcal{G}(x - y)$$



with
retarded
propagator

with
retarded
propagator

Approach initiated long ago: Rosenblum '78 Westpfahl '79, '85 Portilla '80 Bel et al. '81
limited by the technical difficulty of computing the integrals beyond G^2 , ie at $G^2=2$ -loop.

Recently developed to compete with quantum-scattering approach:
Kalin-Porto, Porto et al, Plefka et al, Dlapa-Kalin-Liu-Porto,...

Radiation Reaction and Gravitational Waves at Fourth Post-Minkowskian Order

Christoph Dlapa¹, Gregor Kälin¹, Zhengwen Liu^{2,1}, Jakob Neef^{3,4} and Rafael A. Porto¹ (PRL 10 March 2023)

$$\Delta^{(n)} p_1^\mu = c_{1b}^{(n)} \frac{\hat{b}^\mu}{b^n} + \frac{1}{b^n} \sum_a c_{1\check{u}_a}^{(n)} \check{u}_a^\mu,$$

$$\begin{aligned} \frac{c_{1b}^{(4)\text{tot}}}{\pi} = & -\frac{3h_1 m_1 m_2 (m_1^3 + m_2^3)}{64(\gamma^2 - 1)^{5/2}} + m_1^2 m_2^2 (m_1 + m_2) \left[\frac{21h_2 E^2(\frac{\gamma-1}{\gamma+1})}{32(\gamma-1)\sqrt{\gamma^2-1}} + \frac{3h_3 K^2(\frac{\gamma-1}{\gamma+1})}{16(\gamma^2-1)^{3/2}} - \frac{3h_4 E(\frac{\gamma-1}{\gamma+1})K(\frac{\gamma-1}{\gamma+1})}{16(\gamma^2-1)^{3/2}} + \frac{\pi^2 h_5}{8\sqrt{\gamma^2-1}} \right. \\ & + \frac{h_6 \log(\frac{\gamma-1}{2})}{16(\gamma^2-1)^{3/2}} + \frac{3h_7 \text{Li}_2\left(\sqrt{\frac{\gamma-1}{\gamma+1}}\right)}{(\gamma-1)(\gamma+1)^2} - \frac{3h_7 \text{Li}_2(\frac{\gamma-1}{\gamma+1})}{4(\gamma-1)(\gamma+1)^2} \left. + m_1^3 m_2^2 \left[\frac{h_8}{48(\gamma^2-1)^3} + \frac{\sqrt{\gamma^2-1} h_9}{768(\gamma-1)^3 \gamma^9 (\gamma+1)^4} + \frac{h_{10} \log(\frac{\gamma+1}{2})}{8(\gamma^2-1)^2} \right. \right. \\ & - \frac{h_{11} \log(\frac{\gamma+1}{2})}{32(\gamma^2-1)^{5/2}} + \frac{h_{12} \log(\gamma)}{16(\gamma^2-1)^{5/2}} - \frac{h_{13} \text{arccosh}(\gamma)}{8(\gamma-1)(\gamma+1)^4} + \frac{h_{14} \text{arccosh}(\gamma)}{16(\gamma^2-1)^{7/2}} - \frac{3h_{15} \log(\frac{\gamma+1}{2}) \log(\frac{\gamma-1}{\gamma+1})}{8\sqrt{\gamma^2-1}} + \frac{3h_{16} \text{arccosh}(\gamma) \log(\frac{\gamma-1}{\gamma+1})}{16(\gamma^2-1)^2} \\ & \left. - \frac{3h_{17} \text{Li}_2(\frac{\gamma-1}{\gamma+1})}{64\sqrt{\gamma^2-1}} - \frac{3}{32} \sqrt{\gamma^2-1} h_{18} \text{Li}_2\left(\frac{1-\gamma}{\gamma+1}\right) \right] + m_1^2 m_2^3 \left[\frac{3h_{15} \log(\frac{2}{\gamma-1}) \log(\frac{\gamma+1}{2})}{8\sqrt{\gamma^2-1}} + \frac{3h_{16} \log(\frac{\gamma-1}{2}) \text{arccosh}(\gamma)}{16(\gamma^2-1)^2} + \frac{h_{19}}{48(\gamma^2-1)^3} \right. \\ & + \frac{h_{20}}{192\gamma^7(\gamma^2-1)^{5/2}} + \frac{h_{21} \log(\frac{\gamma+1}{2})}{8(\gamma^2-1)^2} + \frac{h_{22} \log(\frac{\gamma+1}{2})}{16(\gamma^2-1)^{3/2}} + \frac{h_{23} \log(\gamma)}{2(\gamma^2-1)^{3/2}} - \frac{h_{24} \text{arccosh}(\gamma)}{16(\gamma^2-1)^3} + \frac{h_{25} \text{arccosh}(\gamma)}{16(\gamma^2-1)^{7/2}} - \frac{3h_{26} \text{arccosh}^2(\gamma)}{32(\gamma^2-1)^{7/2}} \\ & \left. + \frac{3h_{27} \log^2(\frac{\gamma+1}{2})}{2\sqrt{\gamma^2-1}} + \frac{3h_{28} \log(\frac{\gamma+1}{2}) \text{arccosh}(\gamma)}{16(\gamma^2-1)^2} + \frac{h_{29} \text{Li}_2(\frac{1-\gamma}{\gamma+1})}{4\sqrt{\gamma^2-1}} + \frac{3h_{30} \text{Li}_2(\frac{\gamma-1}{\gamma+1})}{8\sqrt{\gamma^2-1}} \right], \end{aligned}$$

Its PN expansion agrees with Bini-TD-Geralico'23 notably for the $\text{nu}^2 = \mathcal{O}(\text{RR}^2)$ contribution

Current Puzzles

high-energy limits?

G^3 energy loss too large

G^3 angular momentum loss too large (Manohar-Ridgway-Shen'22)

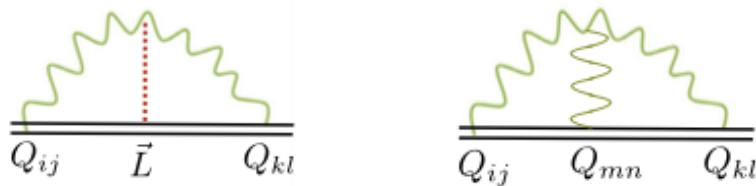
Conservative G^4 scattering diverges

cf ACV motivation: BH formation in HE scattering

Subtleties in defining/computing angular momentum flux (Ashtekar et al., Veneziano-Vilkovisky,...)

low-energy discrepancy at **5PN** between

Foffa-Sturani'19,21,22 Bluemlein et al'21 and Bini-TD-Geralico



**TF-constraint on 5PN $O(\nu^2)$
EFT radiative terms**

$$S_{QQ_L} = C_{QQ_L} G^2 \int dt I_{is}^{(4)} I_{js}^{(3)} \varepsilon_{ijk} L_k$$

$$S_{QQQ_1} = C_{QQQ_1} G^2 \int dt I_{is}^{(4)} I_{js}^{(4)} I_{ij},$$

$$S_{QQQ_2} = C_{QQQ_2} G^2 \int dt I_{is}^{(3)} I_{js}^{(3)} I_{ij}^{(2)}.$$

$$0 = \frac{2973}{350} - \frac{69}{2} C_{QQ_L} + \frac{253}{18} C_{QQQ_1} + \frac{85}{9} C_{QQQ_2}$$

not solved by recent in-in results (Foffa-Sturani'22)

Strong-field scattering of two black holes: Numerical relativity meets post-Minkowskian gravity

Thibault Damour¹ and Piero Retegno^{2,3}

(PRD March 2023)

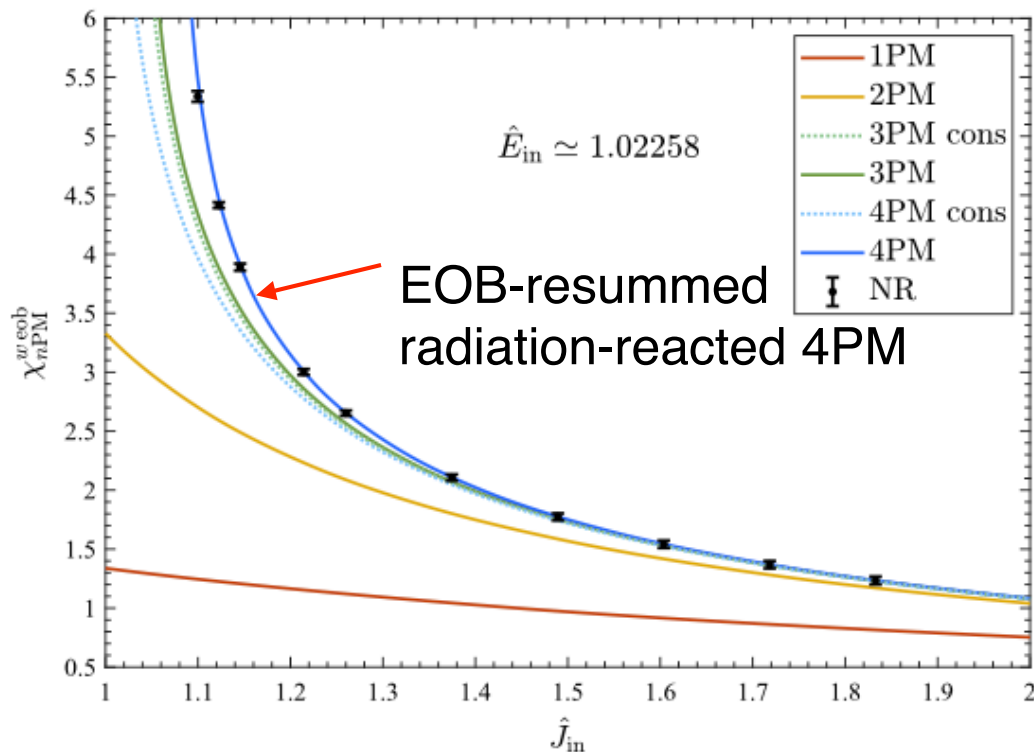
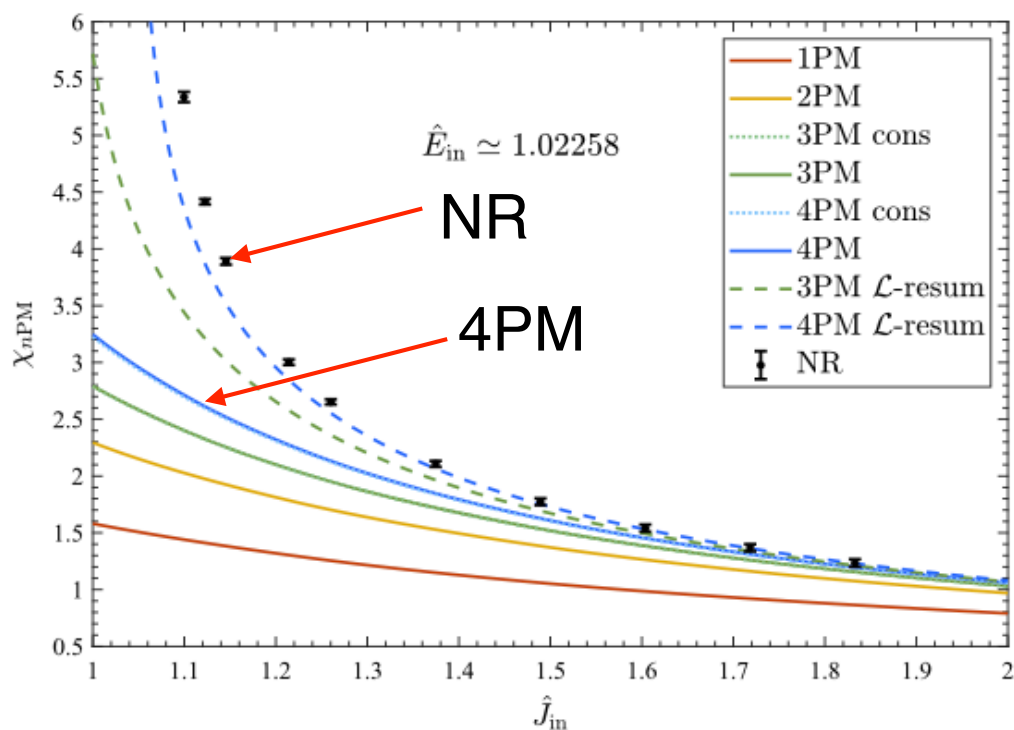
$$\chi_{n\text{PM}}(\gamma, j) \equiv \sum_{i=1}^n 2 \frac{\chi_i(\gamma)}{j^i}$$

$$\mu^2 + g_{\text{eff}}^{\mu\nu} P_\mu P_\nu + Q(X^\mu, P_u) = 0,$$

$$p_{\bar{r}}^2 + \frac{j^2}{\bar{r}^2} = p_\infty^2 + w(\bar{r}, \gamma).$$

$$w(\bar{r}, \gamma) = \frac{w_1(\gamma)}{\bar{r}} + \frac{w_2(\gamma)}{\bar{r}^2} + \frac{w_3(\gamma)}{\bar{r}^3} + \frac{w_4(\gamma)}{\bar{r}^4} + O\left[\frac{1}{\bar{r}^5}\right]$$

$$\chi_{n\text{PM}}^{w\text{eob}}(\gamma, j) \equiv 2j \int_0^{\bar{u}_{\text{max}}(\gamma, j)} \frac{d\bar{u}}{\sqrt{p_\infty^2 + w_{n\text{PM}}(\bar{u}, \gamma) - j^2 \bar{u}^2}} - \pi.$$



PM waveform computation

LO (tree level) waveform

1PM (linearized): Einstein 1918

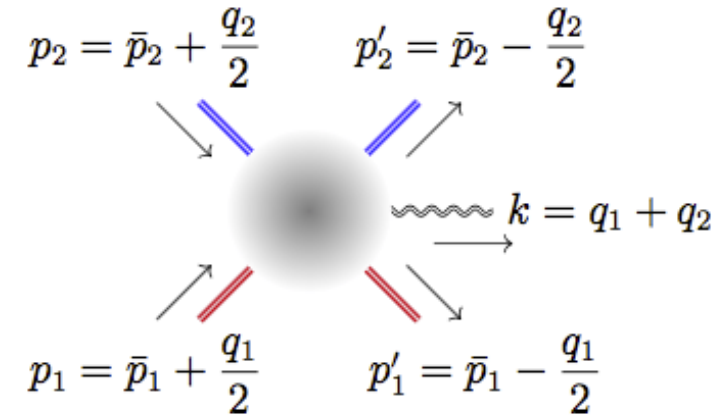
2PM: **classical**: Kovacs-Thorne 1977

quantum-based:

Johansson-Ochirov'15, GoldbergerRidgway'17

Luna-Nicholson-OConnellWhite'18

Mougiakakos-Riva-Vernizzi'21, Bautista-Siemonsen'22



Recent NLO (one-loop) waveform

Andreas Brandhuber^a, Graham R. Brown^a, Gang Chen^b, Stefano De Angelis^c, Joshua Gowdy^a and Gabriele Travaglini^a

Aidan Herderschee,^a Radu Roiban^{b,c} and Fei Teng^{b,c}

Alessandro Georgoudis^a, Carlo Heissenberg^{b,a}, Ingrid Vazquez-Holm^{b,a}

**5-point
amplitude
at one-loop
 $O(G^3)$
waveform**

$$\mathcal{I}_1 := j_{11010} = \text{diagram}$$

$$\mathcal{I}_3 := j_{11011} = \text{diagram}$$

$$\mathcal{I}_5 := j_{11110} = \text{diagram}$$

$$\mathcal{I}_6 := j_{11111} = \text{diagram}$$

$$\mathcal{I}_2 := j_{11100} = \text{diagram}$$

$$\mathcal{I}_4 := j_{11101} = \text{diagram}$$

$$\tilde{\mathcal{I}}_1 := j_{01010} = \text{diagram}$$

$$\tilde{\mathcal{I}}_2 := j_{01011} = \text{diagram}$$

$$\tilde{\mathcal{I}}_4 := j_{01111} = \text{diagram}$$

$$\mathcal{M} = \kappa m_1 \mathcal{M}_1^{\text{lin}} + \kappa^3 m_1 m_2 \mathcal{M}_1^{\text{tree}} + \kappa^5 m_1^2 m_2 \mathcal{M}_1^{\text{one loop}} + (1 \rightarrow 2)$$

$$= -i \frac{\kappa}{2} \epsilon_\mu^* \epsilon_\nu^* \tilde{T}^{\mu\nu}(k) = -i \frac{\kappa}{2} \epsilon_\mu^* \epsilon_\nu^* \int \mu_{12}(q_1, q_2) \tilde{T}^{\mu\nu}(k, q_1, q_2)$$

$$\mu_{1,2}(k) \equiv e^{i(q_1 \cdot b_1 + q_2 \cdot b_2)} \delta^{(4)}(k - q_1 - q_2) \delta(q_1 \cdot u_1) \delta(q_2 \cdot u_2)$$

$$\mathcal{M}_1^{\text{lin}} \quad \tilde{T}_{\text{Fig. 1a}}^{\mu\nu}(k) = \sum_a m_a u_a^\mu u_a^\nu e^{ik \cdot b_a} \delta(\omega_a)$$

$$\tilde{T}_{\text{Fig. 1b}}^{\mu\nu}(k) = \frac{m_1 m_2}{4m_{\text{Pl}}^2} \int_{q_1, q_2} \mu_{1,2}(k) \frac{1}{q_2^2} \left[\frac{2\gamma^2 - 1}{\omega_1 + i\epsilon} q_2^{(\mu} u_1^{\nu)} - 4\gamma u_2^{(\mu} u_1^{\nu)} - \left(\frac{2\gamma^2 - 1}{2} \frac{k \cdot q_2}{(\omega_1 + i\epsilon)^2} - \frac{2\gamma\omega_2}{\omega_1 + i\epsilon} - 1 \right) u_1^\mu u_1^\nu \right],$$

$\mathcal{M}_1^{\text{tree}}$
to be
integrated

$$\tilde{T}_{\text{Fig. 1c}}^{\mu\nu}(k) = \frac{m_1 m_2}{4m_{\text{Pl}}^2} \int_{q_1, q_2} \mu_{1,2}(k) \frac{1}{q_1^2 q_2^2} \left[\frac{2\gamma^2 - 1}{2} q_2^\mu q_2^\nu + (2\omega_2^2 - q_1^2) u_1^\mu u_1^\nu + 4\gamma\omega_2 q_2^{(\mu} u_1^{\nu)} - \eta^{\mu\nu} \left(\gamma\omega_1\omega_2 + \frac{2\gamma^2 - 1}{4} q_2^2 \right) + 2(\gamma q_1^2 - \omega_1\omega_2) u_1^{(\mu} u_2^{\nu)} \right],$$

$\mathcal{M}_1^{\text{one loop}}$

$$\mathcal{M}_{\bar{m}_1^3 \bar{m}_2^2}^{(1)} = \frac{\mathfrak{D}_{\text{IR}}}{\epsilon} + \mathfrak{R} + i\pi \mathfrak{i}_1 + \frac{i\pi}{\sqrt{\bar{y}^2 - 1}} \mathfrak{i}_2 + c_{1,0} \mathcal{I}_1 + c_{2,0} \mathcal{I}_2$$

complicated
rational functions
of 8 variables
with spurious poles

$$+ \mathfrak{l}_{\bar{w}_1} \log \frac{\bar{w}_1^2}{\mu_{\text{IR}}^2} + \mathfrak{l}_{\bar{w}_2} \log \frac{\bar{w}_2^2}{\mu_{\text{IR}}^2} + \mathfrak{l}_q \log \frac{q_1^2}{q_2^2} + \mathfrak{l}_{\bar{y}} \frac{\log \left(\sqrt{\bar{y}^2 - 1} + \bar{y} \right)}{\sqrt{\bar{y}^2 - 1}} + \mathcal{O}(\epsilon^0)$$

Conclusions

- Analytical approaches to GW signals play a crucial role (in conjunction with Numerical Relativity simulations) for the detection, interpretation and parameter estimation of coalescing binary systems (BBH and BNS). It is important to further improve our analytical knowledge for future GW detectors: second generation ground-based detectors, space detectors, second generation ground-based detectors.
- **Quantum (and classical) scattering approaches have given new results of great conceptual interest**, and also of potential interests for GW detection. The **fruitful dialogue** between QFT, EFT, PN, PM, EOB, Tutti-Frutti methods must be vigorously pursued. **Discrepancies must be resolved to complete the determination of the 5PN dynamics (of direct utility for LIGO-Virgo)**. Radiative effects are still puzzling. **Quantum PM waveform computations are promising (though their G-accuracy wont compete with MPM)**.



Henri Poincaré

«Il n’y a pas de problèmes résolus,
il y a seulement des problèmes
plus ou moins résolus »

«There are no (definitely) solved
problems, there are only
more or less solved problems »

